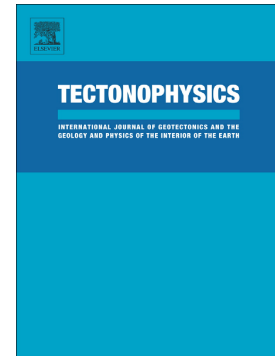# Accepted Manuscript

Constraints on the Neogene growth of the central Patagonian Andes at the latitude of the Chile triple junction (45–47°S) using U/Pb geochronology in synorogenic strata

Andrés Folguera, Alfonso Encinas, Andrés Echaurren, Guido Gianni, Darío Orts, Víctor Valencia, Gabriel Carrasco

Constraints on the Neogene growth of the Central Patagonian Andes at the latitude of the Chile triple junction (45-47°S) using U/Pb geochronology in synorogenic strata

Andrés Folguera[1], Alfonso Encinas[2*], Andrés Echaurren[1], Guido Gianni[3], Darío Orts[4], Víctor Valencia[5], Gabriel Carrasco[6]

1 *Instituto de Estudios Andinos, Universidad de Buenos Aires-CONICET, Argentina.*

2 *Departamento de Ciencias de la Tierra, Facultad de Ciencias Químicas, Universidad de Concepción, Chile.*

3 *Universidad de San Juan, Instituto Volponi-CONICET, Argentina.*

4 *Instituto de Investigación en Paleobiología y Geología. Universidad Nacional de Río Negro – CONICET, Argentina.*

5 *School of the Environment, Washington State University, Pullman, Washington 99164, USA*

6 *Servicios Científicos Educativos y Turismo Científico Chile, Pedro León Ugalde 254, Santiago, Chile.*

* Corresponding author: Alfonso Encinas, aencinas@udec.cl

ABSTRACT

Desertification of Central Patagonia began between ~14-12 Ma and therefore was not directly connected to the opening of the Drake Passage and initial conformation of the Antarctica ice cap in early Miocene times. Local processes, in particular the uplift of the Southern Andes, seem to have played a major role in climatic and biotic changes. We studied synorogenic strata filling a partly cannibalized foredeep between ~45° and 47°S at the latitudes of the Chile triple juction. Older synorogenic successions have yielded 18.7-16.4 Ma (U-Pb) in the western sector of the North Patagonian Cordillera corresponding to Meseta Guadal, Jeinemeni and Alto de Río Cisnes sections. This uplift was partly contemporaneous with broken foreland deformation associated with the San Bernardo fold belt to the east at 17.7-15 Ma. Younger synorogenic successions of 13.5 Ma (U-Pb), associated with a short pulse of major uplift that gave way to deposition of a thick conglomeratic succession, and subsequently finer-grained deposits of 12.3 Ma, are on the eastern Andean front in the Chalía and Guenguell sections, implying a retraction in orogenic activity, and out-of-sequence growth of the Patagonian Cordillera. Consequently, contractional deformation in this area ended after ~12 Ma, sealed by the extrusion of extensive alkali flood basalts, indicating that Neogene shortening only lasted ~6 My, ending around 6 My before the subduction of the Chile Ridge at the latitudes of Central Patagonia and 4.5 My before subduction at the southern tip of South America.

2

1. INTRODUCTION

The Andean Cordillera is the longest and highest elevation orogenic system associated with a subduction setting. This mountain chain has been considered as the archetypical example of the "Chilean-type subduction mode", characterized by contractional deformation related to the strong mechanical coupling between upper and lower plates (Uyeda and Kanamori, 1979). However, the Andean margin has not been in a continuous state of contraction, since there is geological evidence indicating that tectonic shortening alternated with intervals characterized by neutral regimes or extension (e.g., Mpodozis and Ramos, 1990; Jordan et al., 2001; Encinas et al., 2016; Horton and Fuentes, 2016). The Andean Cordillera also shows remarkable geologic and topographic latitudinal differences. The causes of temporal and latitudinal variations are not well understood and have been ascribed to different controls, such as the convergence rate (e.g., Pardo-Casas and Molnar 1987), the absolute westward motion of South America (e.g., Silver et al. 1998), variations in the interplate coupling (Lamb and Davis 2003; Yáñez and Cembrano, 2004), or modifications in the angle of the subducting slab (e.g., Jordan et al, 1983; Muñoz et al., 2000; Martinod et al., 2010; Orts et al., 2015)

Subduction of oceanic active ridges beneath a continent has been characterized as relevant to the geological evolution of the margin, as they represent first-order heterogeneities that affect the tectonic and magmatic development of the upper plate (Scalabrino et al., 2010). In this regard, the region of South America located between ~45 and 47° S is a unique natural

laboratory to study this process, given the present subduction of the Chile Ridge that defines a Chile triple junction (CTJ) between the Nazca, South American, and Antarctic plates (Cande and Leslie, 1986, Figure 1). After the first collision of the Chile Ridge 14 My ago at the southern tip of South America, the CTJ migrated northwards until it reached its present location at the Taitao Peninsula at ~46°S (Cande and Leslie, 1986). The principal geological effects caused by this collision are: 1) the active opening of an asthenospheric slab window below the South American plate that triggered the eruption of extensive flood basalts (Ramos and Kay, 1992; Espinoza et al., 2005; Guivel et al., 2006); 2) subduction erosion of the forearc (Bourgois et al., 1996); 3) the tectonic emplacement of the Taitao ophiolite (Mpodozis et al., 1985; Guivel et al., 1999); 4) near-trench felsic and MORB-like magmatism (Mpodozis et al., 1985); 5) the absence of contemporaneous calcalkaline arc volcanism (Lagrabielle et al., 2007); 6) adakite-like rocks emplacement (Kay et al., 1993).

A point of debate, however, is the spatio-temporal relationship between the Chile Ridge collision and the rapid mountain uplift and fold-thrust belt development in the Patagonian Andes. Some authors have linked this subduction with a contractional episode (Ramos, 1989; Ramos and Kay, 1992; Flint et al., 1994; Gorring et al., 1997; Ramos, 2005), associated with crustal weakening by high heat flow, while others were more conservative about the cause-and-effect relationship between these two processes (Ray, 1996; Suárez and de la Cruz, 2000). In fact, Suárez et al. (2000), Lagabrielle et al. (2007), and Scalabrino et al. (2009, 2010) proposed that the main result after Chile Ridge subduction has not been compressional deformation but instead a fast regional uplift related to slab window mantle driven flow followed by extensional/transtensional tectonism.

4

In the transitional zone from the North to the Austral Patagonian Andes at ~47° S (see Figure 1; Central Patagonian Andes), scarce Cenozoic strata are preserved due to a strong glacial erosion in the last 6 Ma and rapid isostatic uplift linked to the incipient slab window associated with the subduction of the Chile Ridge (Ray, 1996; Suárez and De La Cruz, 2000; Lagabrielle et al., 2004; Ramos and Ghiglione, 2008; Thomson et al., 2010; Guillaume et al., 2013; Herman and Brandon, 2015).

Deposition of these strata followed the onset of a marine transgression that covered most of Patagonia during the early Miocene (Ramos, 1982a). The continental synorogenic deposits formed successions up to 1,200 m thick in the eastern flank of the Patagonian Andes and in the extra-Andean region to the east, where they reached the Atlantic coast of Argentina (Suárez and De La Cruz, 2000; Cuitiño et al., 2016).

In order to understand the geologic evolution of the Patagonian Andes we studied early-middle Miocene synorogenic continental strata in the Andean Cordillera and the western extra-Andean region between latitudes 45-47°S because 1) this is the area where the Chile Ridge is currently subducting, 2) there are good exposures of lower-middle Miocene synorogenic continental strata in the area located between the eastern flank of the Andes and the western extra-Andean region, and 3) this region includes the Meseta Guadal syncline, an isolated exposure of Cenozoic strata surrounded by Paleozoic and Mesozoic rocks that constitutes the only location where Miocene synorogenic deposits have been preserved in the Main Cordillera (Figure 2). In addition, the continental strata of Meseta Guadal overlie lower

Miocene strata deposited during a marine transgression of the Atlantic that reached the axis of the Cordillera at these latitudes. Thus, the basal strata of the terrestrial succession reflect the onset of Andean growth during the Neogene tectonic phase.

Based on new structural and stratigraphic observations and geochronology of growth strata geometries in Neogene deposits, we identified the timing and extent of tectonic structures that were responsible for crustal shortening and topographic uplift of the Central Patagonian Andes. We propose that this phase of deformation was responsible for the orographic rain shadow effect to the east of this mountain belt.

Synorogenic strata associated with the Patagonian Andes uplift, and presently incorporated into the frontal part of the fold and thrust belt, record a major change in isotopic ratios that has been interpreted as reflecting initial desertification of Patagonia at 16.5 Ma (Blisniuk et al., 2005). However, abundance of paleosoils and fauna could indicate prevailing humid conditions at least until ~14.8 Ma (Marshall, 1990; Marshall and Salinas, 1990; Bellosi et al., 2014; Bobé et al., 2015). Additionally, there is a general consensus among different studies that middle to late Miocene (since ~16-15 Ma) was the onset of profound changes in biota and life diversity in central Patagonia as a function of Andean uplift, passing from forest-dominated environments to steppe dominated (see Palazzesi and Barreda, 2012). Then, a final desertification is thought to have occurred after 6 Ma when the Patagonian Andes glaciated as a consequence of rapid isostatic uplift during the opening of a slab window associated with the subduction of the Chile mid ocean Ridge (Figure 1) (Guillaume et al., 2013; Palazzesi et al., 2014).

We document and date synorogenic strata cannibalized in the deformational front of the Patagonian Andes at the latitudes of the present CTJ. Our new radiometric age constraints, together with previously published ages, imply an in-sequence development followed by out-of-sequence deformation of the Patagonian Cordillera that likely determined the climatic conditions prevailing in central Patagonia since 16.5-14.8 Ma analyzed in previous works (Blisniuk et al., 2005; Palazzesi and Barreda (2012; Bobé et al., 2015). Then, we compare these results with previous evolutionary schemes proposed for the Northern Patagonian Andes (~43°S) with the aim of establishing similarities and differences (Orts et al., 2012, 2015; Bilmes et al., 2013; Ramos et al., 2015). Finally, these data allow discussing the potential relationship between the Chile Ridge collision and the uplift of the Southern and Central Patagonian Andes.
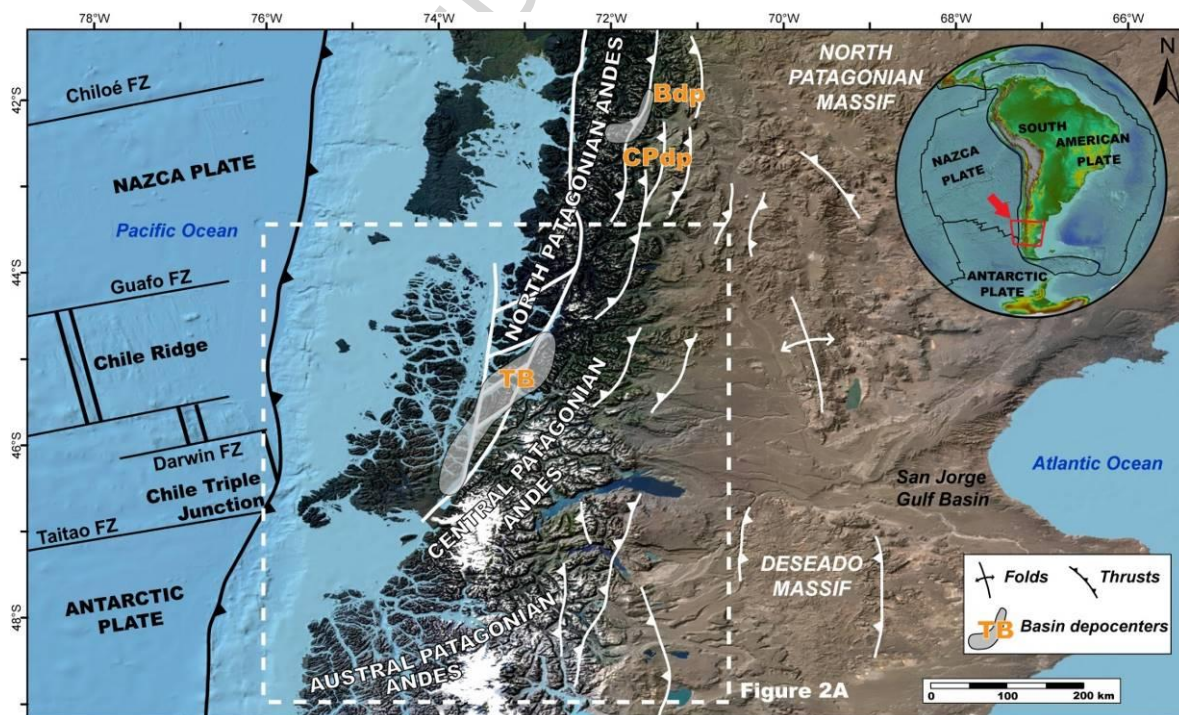

7

Figure 1. *Shaded relief satellite image showing the location of the triple junction point (CTJ) between the South American, Nazca and Antarctic plates and morphostructural units of Patagonia. White lines indicate main structures of the Andean fold-thrust belt and the broken foreland system.TB: Traiguén Basin, CPdp: Cerro Plataforma depocenter, Bdp: El Bolsón depocenter.*

2. GEOLOGICAL AND TECTONIC BACKGROUND

The occurrence of a N-trending, dextral transpressive fault system referred to as the Liquiñe-Ofqui Fault Zone (LOFZ) (Figures 1 and 2), extends ~1,000 km to the north of the CTJ, individualizing a microplate through the present arc front (Hervé, 1994). Cretaceous and Miocene-Pliocene phases of exhumation are recorded through the Patagonian Andes by fission track data (Thomson et al., 2001, 2010, Thomson 2002; Savignano et al., 2016); while exhumation on the eastern Andean front is determined through recognition and dating of synorogenic strata with late Early-Late Cretaceous, early Eocene and Neogene ages (Orts et al., 2012; Bilmes et al., 2013; Ramos et al., 2015; Gianni et al., 2015, 2017; Echaurren et al., 2016). These events are separated by an episode of extension that started in the late Eocene (Paleocene?) and peaked in the late Oligocene-early Miocene (Muñoz et al., 2000; Aragón et al., 2011; Orts et al., 2012, 2015; Encinas et al., 2015; Gianni et al., 2017).

In the transition zone between the North and Austral Patagonian Andes, the crystalline basement is composed of Carboniferous metamorphic rocks of the Eastern Andean Metamorphic Complex (Figure 2) (see Hervé et al., 1994), covered by tholeiitic to calc-

alkaline volcanic rocks of the Ibáñez-Lago La Plata formations, emplaced under a Mid-Late Jurassic extensional regime (Skarmeta, 1976; Ramos, 1976; Echaurren et al., 2016). At the top, these volcanic rocks are interfingered with the marine Coyhaique Group, a transgressive to regressive sedimentary sequence with Early Cretaceous ages that underlies the Aptian-Albian volcanic rocks of the Divisadero Group (Figure 2) (Skarmeta, 1976; Ramos, 1976). The latter contact relationship has been identified as uncomformable, denoting a late Early Cretaceous stage of deformation that affected both the cordilleran realm as the Patagonian intraplate area (Folguera and Iannizzotto, 2004; Gianni et al., 2015; Echaurren et al., 2016).

The scarce Cenozoic record in this region is conformed by isolated depocenters, mostly along through the edges of the mountainous area. The Cenozoic Traiguén Basin (Figures 1 and 2) consists in tholeitic basalts interfingered with deep marine sediments of 26-23 Ma, presently exhumed at the western Andean front, which represents highly attenuated conditions for the continental crust (Hervé et al., 1995; Encinas et al., 2015). To the north, the Cerro Plataforma depocenter hosts marine deposits of ~18.5 Ma, which have been interpreted as the inception of a foreland basin due to the recognition of syncontractional growth strata (Orts et al., 2012). Younger synorogenic sedimentation is deposited in isolated depocenters to the east of the Main Andes with ages that sparce between 16.1 and 12 Ma (Bilmes et al., 2012, 2013; Bechis et al., 2014; Ramos et al., 2015).

To the south, the Meseta Guadal has the most complete Cenozoic record with late Paleocene to Eocene fluvial sections of the Ligorio Marquez and San José formations, whose ages have been determined on the basis of fossil flora (Troncoso et al., 2002; De la Cruz and Suárez,

9

2006) (Figure 2). These strata are conformably covered by marine sediments of the Guadal Formation. These exposures of the Guadal Formation constitute the westernmost outcrops of these marine rocks with a probable Atlantic provenance (Flynn et al., 2002; Suárez et al., 2007), correlative to the Patagoniano Formation in the extra-Andean region. These marine rocks were assigned on the basis of fossils and Sr ages to the upper Oligocene-lower Miocene (Frassinetti and Covacevich, 1999; Cuitiño et al., 2012, 2015a, b). Overlying these strata, the continental deposits of the Santa Cruz Formation bear a diverse mammal fauna, assigned to the early Miocene (Flynn et al., 2002).

Additionally, Lagabrielle et al. (2004) and Suárez et al. (2007) described progressive unconformities for the Miocene Santa Cruz Formation at Meseta Guadal indicating its synorogenic character.

On the eastern Andean mountain front to the east, younger sequences of the Río Frías and El Oscuro, Pedregoso and Río Mayo formations, covering lower Miocene and locally Eocene sections (Rivas et al., 2015; Dal Molin and Franchi, 1996), have been dated by Ar/Ar at the mid to upper Miocene and were related to a last stage of mountain growth in the North Patagonian Andes (Marshall, 1990).
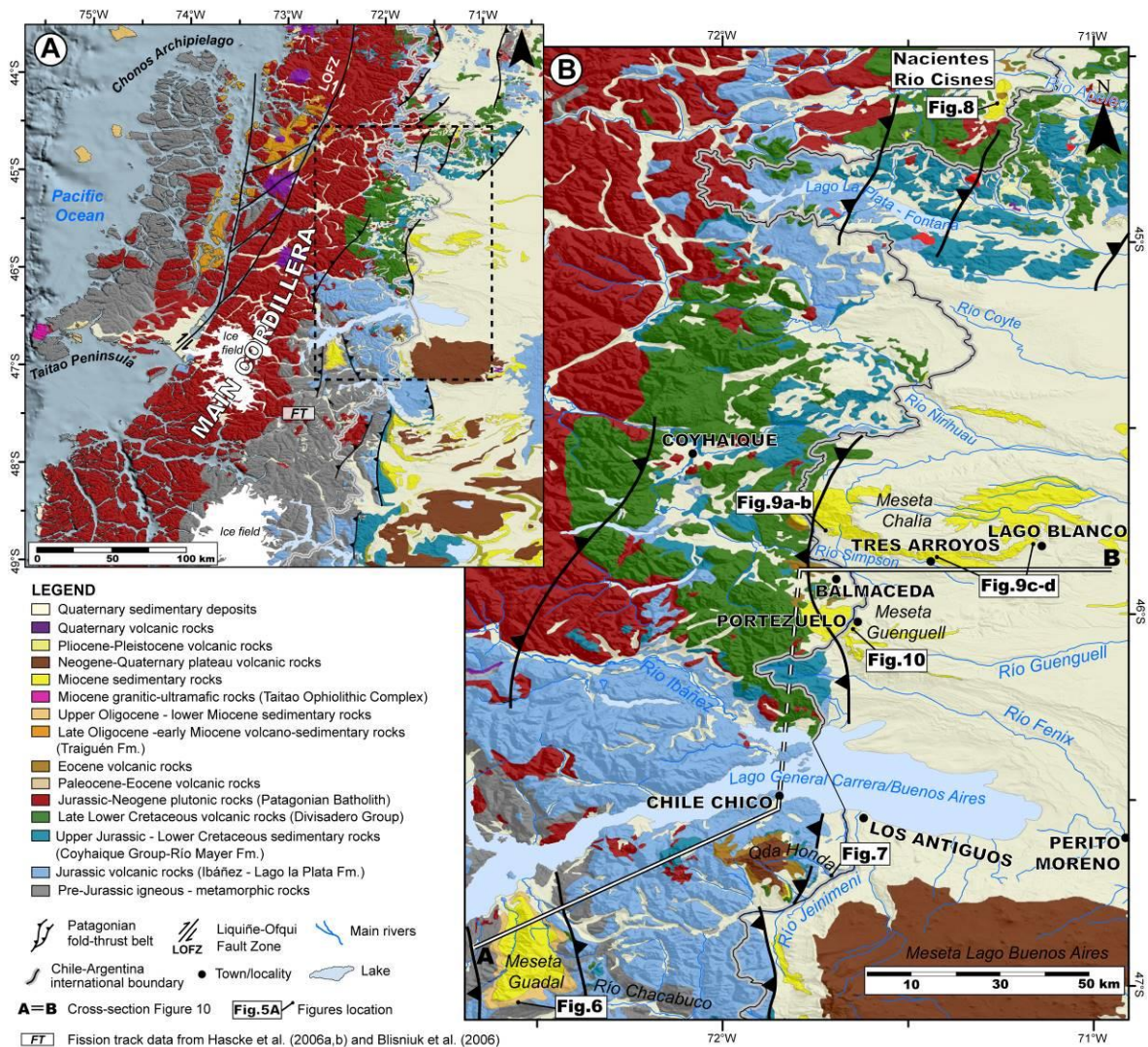
Figure 2. *A) Geological map of the Patagonian margin in the vicinity of the Chile Triple Junction (CTJ). Note the scarceness of Neogene deposits along the axial part of the Andes, mainly circumscribed to Traiguén Island and to the eastern cordilleran front. B) Study area and location of the points of sampling on synorogenic sequences. A-B transect corresponds to an evolutionary scheme shown in Figure 11. Maps based on Ploszkiewicz and Ramos (1977), González (1978), Sernageomin (2003), De La Cruz et al. (2003a, b), De La Cruz and Suárez (2008), Suárez et al. (2007).DEM correspond to SRTM from NASA.*

3. MIOCENE CONTINENTAL STRATA BACKGROUND

3.1 Meseta Guadal area

The Meseta Guadal (also known as the Meseta Cosmelli) is a syncline bounded by reverse faults of opposing vergence directions that is located in the Andean Cordillera between the Lago General Carrera and the Río Chacabuco (~47°S) (Figure 2). Here, Cenozoic sedimentary rocks overlie Paleozoic metamorphic rocks of the Eastern Andean Metamorphic Complex and Jurassic to Cretaceous volcanic and sedimentary rocks of the Ibáñez and El Toqui formations (De la Cruz et al., 2004; De la Cruz and Suárez, 2008).

The Cenozoic rocks consist on a concordant succession of Lower Paleogene fluvial deposits of the Ligorio Márquez and San José formations, upper Oligocene-lower Miocene marine strata of the Guadal Formation (De la Cruz and Suárez, 2008), and lower Miocene fluvial strata, with a not yet resolved formal designation (see discussion in Flynn et al., 2002), which are the focus of our study in this area. The succesion was defined as the Río Zeballos Formation by Niemeyer (1975), Galera Formation by Niemeyer et al. (1984), Santa Cruz Formation by De la Cruz et al. (2004), and Pampa Castillo Formation by Scalabrino (2009). Because correlation of these units is still dubious, we prefer to use the local name of Pampa Castillo Formation that refers to the homonimous locality in the southern part of the Meseta Guadal syncline (Figure 2). This ~1000 m thick unit, gradationally overlies the marine strata of the Guadal Formation but its upper limit is not exposed (De la Cruz et al., 2004; De la Cruz and Suárez, 2008). The Pampa Castillo Formation consists of siltstone, sandstone and conglomerate (Niemeyer, 1975; De la Cruz et al., 2004; De la Cruz and Suárez, 2008) and

contains fossils of vertebrates, poorly preserved leaves, trunks, and freshwater bivalves (Flynn et al., 2002; De la Cruz and Suárez, 2008; Bostelmann and Buldrini, 2012). The lower part of this unit was deposited in a high sinuosity fluvial environment, whereas the upper part represents low sinuosity fluvial conditions (Flint et al., 1994). De la Cruz and Suárez (2008) reported transport from WNW to ESE from paleocurrents analysis, and possible growth-strata geometries approximately in the middle part of the Pampa Castillo Formation. The vertebrate fauna of the Pampa Castillo Formation was assigned to the Santacrucian SALMA (South AmericanLand Mammal Age) by Flynn et al. (2002) and Bostelmann and Buldrini (2012) and to the Pinturian SALMA by Chick et al. (2010) (Figure 3).

3.2 Jeinemeni area

Miocene continental deposits crop out south of the Lago General Carrera and north of the Lago Posadas, in both sides of the Jeinemeni River (which marks the international border between Chile and Argentina, Figure 2) at ~47° S (Ray, 1996; Lagabrielle et al., 2004). These strata were defined as the Río Zeballos Formation by Niemeyer (1975), the Galera Formation by Niemeyer et al. (1984) and Ray (1996) (who divided this formation in a lower and an upper unit), and the Santa Cruz Formation by De La Cruz and Suárez (2008) in Chile (west of the Jeinemeni River) (Figure 3). For the same deposits in Argentina, east of the Jeinemeni river, a more refined stratigraphic scheme had been proposed earlier by Ugarte (1956), defining the Río Zeballos Group, dividing it into the Río Jeinemeni, Cerro Boleadoras, and Río Correntoso formations (see also Escosteguy et al., 2002, 2003). The Río Zeballos Group is exposed at the edges of the Meseta Lago Buenos Aires, the Jeinemeni River and other

valleys and creeks in the area (Figure 2). The westernmost extent of this unit is delimited by a reverse fault that has an approximate N-S orientation and marks the limit between the Patagonian Cordillera and the Meseta Lago Buenos Aires to the east (Figure 2) (Ray, 1996; Lagabrielle et al., 2004; De la Cruz and Suárez, 2008). East of this fault, the Río Zeballos Group transitionally overlies the upper Oligocene-lower Miocene marine strata of the Guadal Formation and unconformably underlies the late Miocene-Pliocene basalts of the Meseta Lago Buenos Aires Formation (Figure 3) (Escosteguy et al., 2003; Guivel et al., 2006).

West of the Jeinemeni Fault (De la Cruz and Suárez, 2008), the Río Zeballos Group does not crop out and the Meseta Chile Chico upper basalts, equivalent to the Meseta Lago Buenos Aires basalts, directly overlie the Guadal Formation (Figures 2 and 3) (Espinoza et al., 2005; De la Cruz and Suárez, 2008). The Río Zeballos Group consists of an upward coarsening succession up to ~1,200 m thick of sandstones, siltstones, mudstones, conglomerates, and tuffs that contain abundant vertebrate fossils (Dal Molin and Colombo, 2003; Lagabrielle et al., 2004), and it is capped by andesitic to basaltic calc-alkaline rocks of the Zeballos Volcanic Sequence (Espinoza et al., 2010). The Río Zeballos Group shows, from base to top, facies characteristic of lacustrine, deltaic, and alluvial systems according to Dal Molín and Colombo (2003), and associated with a meandering fluvial system as interpreted by De la Cruz and Suárez (2008). In its lower part, growth strata associated with folds and thrusts have been described (Ray, 1996; Lagabrielle et al., 2004). The age of the Río Zeballos Group remains elusive. The Cerro Boleadoras Formation contains vertebrate fossils that were respectively assigned to the Santacrucian SALMA (lower Miocene) by Carlini et al. (1993) and Vucetich (1994) and to the Friasian SALMA (upper lower to middle Miocene) by

14

Scillato et al. (1993) (see Figure 3). Espinoza et al. (2010) obtained four K/Ar ages between ~16 and 14 Ma for the Zeballos Volcanic Sequence in the top of the Río Zeballos Group (see Figure 3).

3.3 Alto Río Cisnes area

The Río Frías Formation is a continental succession that was defined at the Alto Río Cisnes (~44°30'S, Chile), next to the drainage divide between Chile and Argentina (Figure 2). This succession was first studied by Roth in 1897-1898, although Ploszkiewicz and Ramos (1977) and Ramos (1981) were the ones to define it as the Río Frías Formation. The Río Frías Formation unconformably overlies Lower Cretaceous volcanic rocks of the Divisadero Group and unconformably underlies a succession of conglomerate and sandstone of unknown age that was correlated with the Galera Formation by De la Cruz and Cortés (2011).

The Río Frías Formation is a 131 m thick succession of tuffs, tuffaceous siltstones, sandstones, and conglomerates (Marshall and Salinas, 1990; De la Cruz and Cortés, 2011), containing abundant fossils of vertebrates, scarce remains of carbonized plants (Ameghino, 1906; Bostelmann et al., 2012a, b; Bobé et al., 2015), and several paleosoil intervals with abundant insect traces that characterize the *Coprinisphaera* ichnofacies (Bostelmann et al., 2012a, b; Bellosi et al., 2014). The Río Frías Formation was deposited in a fluvial environment (Marshall and Salinas, 1990), with abundant tuffs and pyroclastic material that requires the onset of possible nearby explosive volcanism (De la Cruz and Cortés, 2011).

3.4 Meseta de Chalía area

A continental succession of siliciclastic and volcanoclastic deposits is well exposed in the river cuts of the Meseta Chalía (Argentina) and also in some limited outcrops east of Coyhaique (Chile), near the border with Argentina (see Figure 2). Dal Molín and Franchi (1996) modified previous stratigraphic schemes of González (1967, 1978) for the area of Meseta Chalía, Lago Blanco, and Río Mayo (Figure 2) and defined, from base to top, the Río Frías, Pedregoso, Río Mayo, and Chalía formations (Figure 3). The basal unit is a 10 m thick succession of tuffs and siltstones that was tentatively correlated with the Río Frías Formation by Dal Molín and Franchi (1996). The Pedregoso Formation is a fluvial and alluvial succession up to 250 m thick that consists of polymictic conglomerates and minor sandstones (Dal Molín and Franchi, 1996). Franchi et al. (1995) dated a tuff from this unit using the Ar/Ar method and obtained an age of 12.1 Ma. The Río Mayo Formation is a 800 m thick succession of tuffs, tuffaceous siltstones, sandstones, and conglomerates that contains vertebrate fossils and was deposited in fluvial and lacustrine enrironments (Dal Molín and Franchi,1995; Escosteguy et al., 2003). De Iuliis et al. (2008) assigned the vertebrate fauna of this unit to the Mayoan SALMA (Figure 3). The upper Chalía Formation, a succession of more than 400 m in thickness, is composed of gravel and minor sand that was tentatively assigned to the upper Miocene-Pliocene by Dal Malín and Franchi (1995). Because this unit is composed of loose sediment, we do not discard that it could correspond to fluvial deposits related to the Plio-Pleistocene glaciations that occurred in this area.

In the Meseta Chalía-Lago Blanco area, Gianni et al. (2017) dated a tuff from the lower unit defined by Dal Molín and Franchi (1996) at the Arroyo Pedregoso in the la Estancia La Elida with the U-Pb method and obtained an age of 39.8 Ma, which indicates that an Eocene tuff unit is separated from the Pedregoso Formation by a subtle angular unconformity.

In eastern Chile, Skarmeta (1976) grouped all Miocene continental deposits of the area in the Galera Formation and correlated them with the Pedregoso and Río Mayo formations (Figure 3). Subsequently, De la Cruz et al. (2003b) and De la Cruz and Suárez (2006) limited the Galera Formation to a 500 m thick succession of conglomerates and minor sandstones that crop out at the Coyhaique surroundings. They considered this unit as deposited by braided gravel-bed rivers. The Galera Formation was correlated with the Pedregoso Formation by De la Cruz and Suárez (2006) (Figure 3).

3.5 Meseta de Guenguell area

The continental succession of the Meseta Guenguell crops out north of the Lago General Carrera-Buenos Aires and south of Balmaceda in eastern Argentina and western Chile. In the Argentinan sections, Escosteguy et al. (2003) defined, from base to top, the Río Frías, El Portezuelo, Río Mayo, and Chalía formations. The basal unit, 20 m thick, is a succession of tuff and tuffaceous siltstone that was tentatively correlated with the Río Frías Formation by Escosteguy et al. (2003). The El Portezuelo Formation is a 150 m thick succession of sandstone and conglomerate deposited in a fluvial environment that was assigned to the middle Miocene by K/Ar dating of pumice clasts from this unit and correlated with the Galera

17

Formation (Escosteguy et al., 2003). The Río Mayo Formation is a 250 m thick succession of tuff, sandstone, siltstone, and conglomerate deposited in fluvial and lacustrine enrironments (Escosteguy et al., 2003). De Iuliis et al. (2008) studied vertebrate fossils from this unit at Cerro Guenguell and assigned them to the Mayoan SALMA (Figure 3). In addition, they obtained an Ar/Ar age of 11.8 Ma from a tuff of this unit.

Southwest of Balmaceda, in eastern Chile, Ray (1996) defined the Oscuro Formation as a succession of tuff, silstone and sandstone that paraconformably overlies the Eocene Basaltos de Balmaceda Formation, and correlated by De la Cruz et al. (2003a, b) with the Río Frías Formation. However, a recent study by Rivas et al. (2015) divides the Oscuro Formation in different units, i) a basal succession of volcaniclastic sandstones and tuffs of 46.7 Ma (U-Pb), ii) volcaniclastic sandstones and tuffs with lower-middle Miocene vertebrate fossils and iii)-iv) fluvial sandstones and siltstones correlated with the El Portezuelo Formation, constraining the middle part of the sequence to the 12.3-12.1 Ma (U-Pb) interval, and reporting, in unit iv), rests of the vertebrate fossil *Interatheriinae* sp., which constitute the first Mayoan fossil mammal of the Chilean Patagonia (Figure 3).

4. NEOGENE PALEOECOLOGICAL BACKGROWND

At present, the Patagonian Andes form a topographic barrier up to ~4 km to atmospheric circulation that cause one of the most drastic orographic rain shadows on earth (Blisniuk et al., 2005). The humid westerlies coming from the Pacific generate intense rainfall in the western part of the Andes (~3,000 mm/yr) contrasting with only ~200 mm/yr to the east of

this chain. As a consequence, the temperate rainforest in the forearc passes to an open grass-dominated steppe in the extra-Andean region (Barreda and Palazzesi, 2007; Palazzesi et al., 2014). The increase in aridity in the eastern foreland enhanced progressively during the Neogene and was caused by a combination of global cooling and the progressive uplift of the Main Cordillera that caused an important orographic rain shadow to the east of this mountain belt (Barreda and Palazzesi, 2007; Palazzesi and Barreda, 2012).

Fossil evidence indicate an important increase in the aridity of the Patagonian foreland during the middle-late Miocene (Ortiz-Jaureguizar and Cladera, 2006; Barreda and Palazzesi, 2007). Studies based in fossil pollen indicate the rise in importance of shrubby and herbaceous elements since the middle-late Miocene. Rainforest elements typical of the late Oligocene-early Miocene period became rare or extinct toward the late Miocene (Barreda and Palazzesi, 2007). However, the final expansion of the present grass-dominated steppe only took place during the last 6 Myr, following the expansion of ice sheets in Antarctica and the widespread Neogene glaciation of the Patagonian Andes (Palazzesi and Barreda, 2012; Palazzesi et al., 2014). Dunn et al. (2015) calculated variations in leaf area index (the degree of canopy openness) during the Cenozoic based on the study of phytoliths derived from leaf epidermal cells and determined a tendency to a progressively more open vegetation environments since ~14.2 Ma.

Studies based on fossil mammals from Neogene deposits of Patagonia indicate the occurrence of diverse communities composed by grazers, browsers, and frugivorous taxa during the early Miocene, which suggest the presence of woodlands and grasslands (Ortiz-

19

Jaureguizar and Cladera, 2006). During the middle Miocene grazers almost doubled their relative importance, and conversely, frugivorous and browsers reduced their relative diversity, which is consistent with an extensive change from park savanna to grassland and steppe-like environments. The presence of primates in the middle Miocene successions (Bobé et al., 2015), including the Río Frías Formation (dated in 15.8 Ma in Encinas et al., 2016), indicates that warm and forested habitats were still conspicuous at that time (Ortiz-Jaureguizar and Cladera, 2006). Latter in middle Miocene, most of the preceding mammal taxa related to subtropical woodlands became completely extinct (Ortiz-Jaureguizar and Cladera, 2006).

South American Land Mammal ages (SALMA) are unique associations of vertebrate taxa that are inferred to have existed during a restricted interval of time and have been used to subdivide geologic time (Marshall and Salinas, 1990) (Figure 3). However, the occurrence of similar taxa in different faunal associations, the definition of faunal units that only occur in restricted localities (e.g. the Pinturan) and the lack of sufficient radiometric dates, among other problems, have produced controversies (see a thorough discussion in Flynn et al., 2002, 2005). Basically, four faunal units have been defined in Miocene synorogenic strata of Patagonia at the study latitudes, the Notohippidian, Santacrucian, Friasian, and Mayoan (see Figure 3). Cuitiño et al. (2016) bracketed the Notohippidian between ~18.8 and ~18.0 Ma and considered this fauna to be partially synchronous with the more local Pinturan fauna. The Santacrucian was constrained by Flynn and Swisher (1995) to 16.3–17.5 Ma. Later, Perkins et al. (2012) obtained ages between 17.8-16 Ma for the classic Santacrucian localities

in the Atlantic coast of Patagonia. More recently Cutiño et al. (2016) restricted the Santacrucian between ~18.2 to ~15.6 Ma.

Ameghino (1906), proposed the Friasian SALMA as intermediate in age between the Santacrucian and younger faunas. However, Marshall (1990) and Marshall and Salinas (1990) correlated the Friasian and Santacrucian SALMAs (16.3-17.5 Ma according to Flynn and Swisher, 1995), based principally in their study of fossil marsupials from the Alto del Río Cisnes section and an Ar-Ar date of ~17 Ma from this locality (Flynn et al., 1989). Bostelmann et al. (2012a, b) proposed instead that the Río Frías fauna was more similar to the Colloncuran fauna of Argentina dated at 15.7 Ma by Flynn and Swisher (1995). An Ar/Ar age of 14.8 Ma (De la Cruz and Cortés, 2011) and the U-Pb age of 15.8 Ma obtained by Encinas et al., (2016) favors the notion that the Río Frías Formation is younger than the Santa Cruz Formation.

Finally, the Mayoan fauna has been bracketed between 11.8 and 13.3 Ma (Dal Molin and Franchi 1996; Madden et al. 1997; De Iuliis et al., 2008; Dunn et al. 2015).
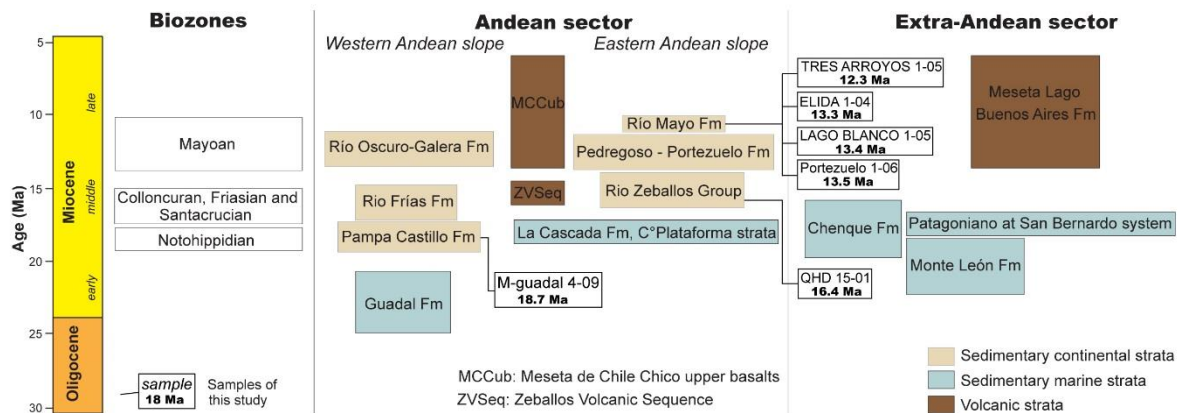

Figure 3. *Biozons and main stratigraphical units discussed in the text (data taken from Ugarte 1956, Niemeyer 1975, 1984, Ploszkiewicz and Ramos 1977, Ramos 1981, Marshall and Salinas 1990, Carlini et al. 1993, Scillato et al. 1993, Vucetich 1994, Ray 1996, Dal Molín and Franchi 1996, Flynn et al. 2002, Escosteguy et al. 2002, 2003, De la Cruz et al. 2004, De la Cruz et al. 2004; Espinoza et al. 2005, 2010; , Lagabrielle et al. 2004, Guivel et al. 2006, De la Cruz and*

21

Suárez 2006, 2008, De Iuliis et al. 2008, Scalabrino 2009, Chick et al. 2010, De la Cruz and Cortés 2011, Bostelmann and Buldrini 2012, Rivas et al. 2015).

5. METHODOLOGY

5.1 U-Pb zircon geochronology

Six samples of approximately 10 kg each were selected for U-Pb zircon geochronology. Zircon crystals were extracted at ZirChron LLC, Tucson AZ by Electro Pulse Disaggregator (EPD) followed by traditional methods. Analytical strategy for zircon analysis consisted in random analysis of grains for both tuffs and sandstones. The rock fragments were placed in the sample chamber of an EPD CNT SPARK-3, and then electrical pulses were applied at 2 Hz repetition and ~250 kV discharges for 15 minutes. The sample materials that passed through the 500 micron stainless steel mesh sieve were collected. The coarser material remaining in the EPD chamber was collected, dried and size reduced by jaw crusher and disk pulverizer. The rock material (<500 microns) was processed following traditional procedures (table concentrator, isodynamic magnetic separator, and heavy liquids).

The general procedure for each sample was first the handpicking of zircons from the non-magnetic fraction under the microscope.

Then the zircons were mounted in a 1-inch diameter epoxy puck and slightly ground and polished to expose the surface and keep as much material as possible for laser ablation analyses. After CL imaging, the LA-ICP-MS U-Pb analyses were conducted at Washington

State University using a New Wave Nd:YAG UV 213-nm laser coupled to a ThermoFinnigan Element 2 single collector, double-focusing, magnetic sector ICP-MS. Operating procedures and parameters are similar to those of Chang et al. (2006). Laser spot size and repetition rate were 30 microns and 10 Hz, respectively. He and Ar carrier gases delivered the sample aerosol to the plasma. Each analysis consists of a short blank analysis followed by 250 sweeps through masses 202, 204, 206, 207, 208, 232, 235, and 238, taking approximately 30 seconds. Time-independent fractionation was corrected by normalizing U^{238}/Pb^{206}, U^{235}/Pb^{207} and Pb^{207}/Pb^{206} ratios of the unknowns to the zircon standards (Chang et al., 2006). U and Th concentration were monitored by comparing to 91500 zircon standard (Wiedenbeck, et al., 1995).

Two zircon standards were used: Plesovice, with an age of 338 Ma (Slama et al., 2008) and Fish Canyon Tuff, with an age of 28.4 Ma (Schmitz and Bowring, 2001). Common Pb corrections were using the 207Pb method (Williams, 1998).Uranium-lead ages were calculated using Isoplot (Ludwig, 2003).

U–Pb zircon crystallization age's errors are reported using quadratic sum of the analytical error plus the total systematic error for the set of analyses (Valencia et al., 2005).

We analyzed six samples from sandstone and tuff strata of different Neogene units in the Central Patagonian Andes at ~45-46° S. Results from the LA-ICPMS zircon U-Pb isotope analyses of these samples are presented in Table DR1. In order to determinate the maximum depositional ages, ~45-100 zircon crystal per sample were analyzed.

Calculated maximum depositional for $^{206}U/^{238}Pb$ Tuff Zirc ages are in Table 1, and probability density of age distribution and Tuffzirc age plots are shown in Figure 4.

Zircons from these samples are clear and colorless and display a variety of morphologies, but mainly are long euhedral crystals dominated by long, prominent pyramidal terminations subordinate are subhedral morphologies.

As observed through cathode-luminescence (CL), zircons generally consist of simple oscillatory to sector zoning.

5.2 Identification of growth strata

We visited classical localities (see Niemeyer, 1975; Marshall and Salinas, 1990; Dal Molín and Franchi, 1996; Ray, 1996; Ecosteguy et al., 2003; Lagabrielle et al., 2004; De la Cruz and Suárez, 2006; 2008) at the transitional zone between the northern and southern Patagonian Andes looking for Miocene synorogenic strata. We present new data of internal angular unconformities, condensed sequences, onlap relations and fanning strata arrangements associated with contractional structures, in the Alto Río Cisnes, Jeinemeni, Meseta de Guenguell and Meseta de Chalía areas of both Andean slopes (see Figure 2). We sampled strata in these areas for U-Pb dating of their detrital components.

6. RESULTS

6.1 U-Pb zircon geochronology

All the samples, corresponding to Meseta Guadal-Cosmelli, western Meseta Guenguell, Meseta Chalía, and Jeinemeni and Río Cisnes headquarters (Figure 2), yielded Cenozoic maximum depositional ages (12.3-18.7 Ma) with different proportions of older age components (Table 1, table DR1, and Figures 4 and 5), being the Early Cretaceous peak the most distinctive. Meseta Guadal-Cosmelli sample (Sample MGuadal 4.09) yielded an early Miocene maximum depositional age (18.7 ±0.3 Ma, 2σ, n=42) and has an older component ranging from Miocene to Neoproterozoic (20-623 Ma), with a minor Oligocene age cluster (28-32 Ma, n=4) and an Early Cretaceous component (98-130 Ma, n=6). Río Jeinemeni sample (Sample QHD 15.1) yielded a maximum depositional age of 16.4 +0.2/-0.3 Ma (2σ, n= 104) with a significant Oligocene age peak (27-33 Ma, n=16) and a Cretaceous component (84-128 Ma, n=12). Western Meseta Chalía sample (Sample Elida 1.04) has a maximum depositional age of 13.3 ±0.2 Ma (2 σ, n=44), and two zircon grains have older ages (87 and 170 Ma). A sample near the top of the Meseta Chalía (Sample Tres Arroyos 1.05) yielded a Miocene maximum depositional age (12.3 ±0.3 Ma, 2 s, n=19) and has an important cluster of ~15 Ma, and Cretaceous zircons distributed between 88-111 Ma. A sample located to the south of Meseta Chalía and near Lago Blanco locality (Sample Lago Blanco 1.05) yielded a maximum depositional age of 13.4 ±0.2 (2 σ, n=42) in 100 analyses, and also has a Miocene age cluster (~15 Ma) and a Cretaceous age peak (>10%, ~92-107 Ma). In a sample from the western Meseta Guenguell (Portezuelo 1.06 sample), only 45 grains were analyzed, which yielded a 13.5 +0.3-0.5 Ma maximum depositional age (2σ, n=22) and also have a Mesozoic age component (94-148 Ma).

Sample	Maximum Age of Deposition 206Pb/238U Ma	Other ages (Ma)
- MGuadal 4.09.	18.7 ±0.3	~28-32 (n=4), 98-130 (n=6), 303, 368, 424, 623
- QHD 15-1.	16.4 +0.2/ -0.3	~27-33 (n=16), 84-128 (n=12), 167
- Elida 1.04.	13.3 ±0.2	87 and 170
-Tres Arroyos 1.05.	12.3 ±0.3	~15 (n=11), 88-111 (n=17)
- Lago Blanco 1.05.	13.4 ±0.2	~15 (n=27), 92-107 (n=17)
- Portezuelo 1.06.	13.5 +0.3/-0.5	~94-148 (n=16)

Table 1. *Detrital zircon data obtained for the collected samples (see Appendix).*

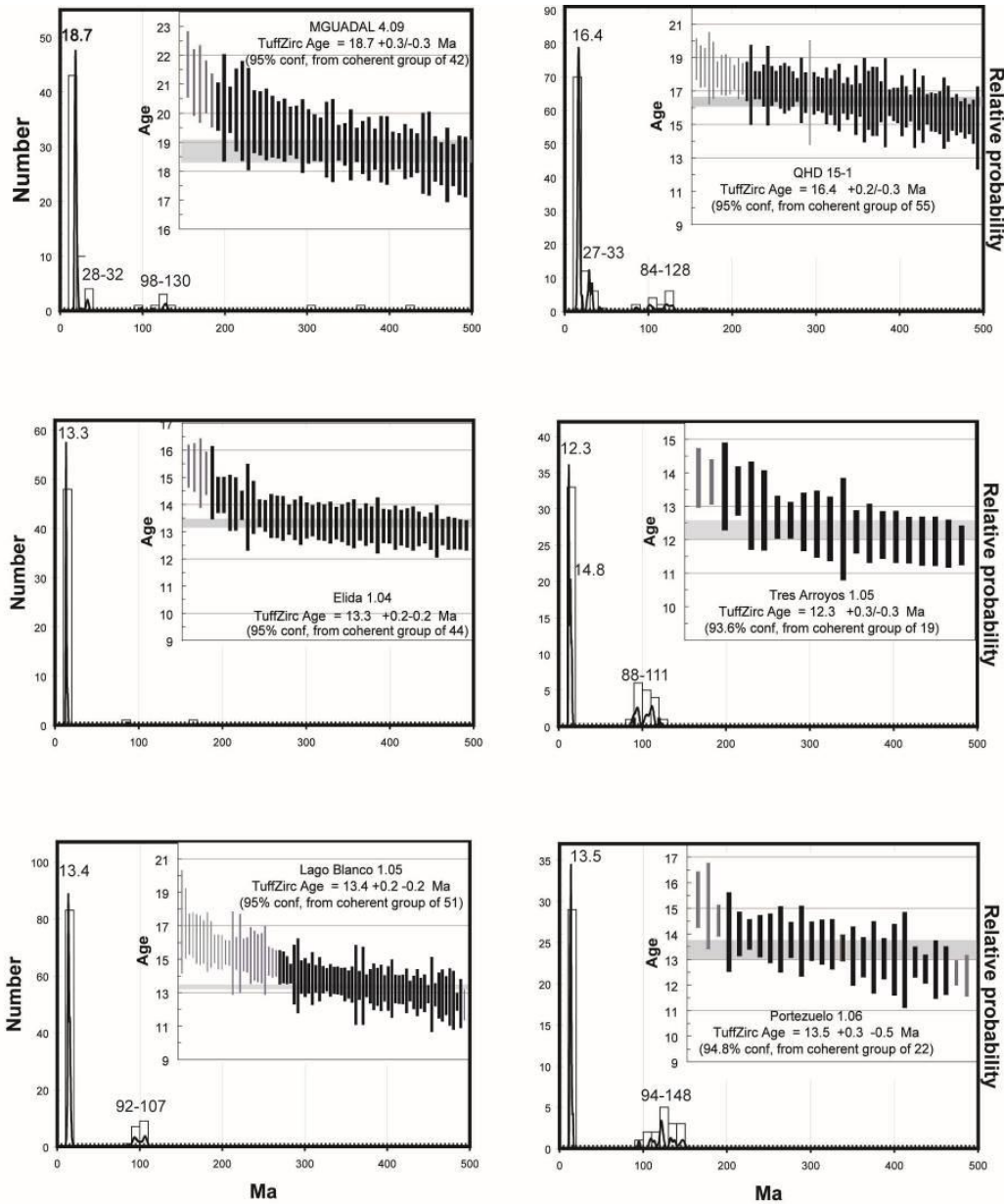**Figure 4.** *U-Pb ages and probability density plots for reworked tuffs and one primary tuff (Elida 1-04) of the different Miocene synorogenic units studied in this work. Grey bars represent maximum depositional age rank.*
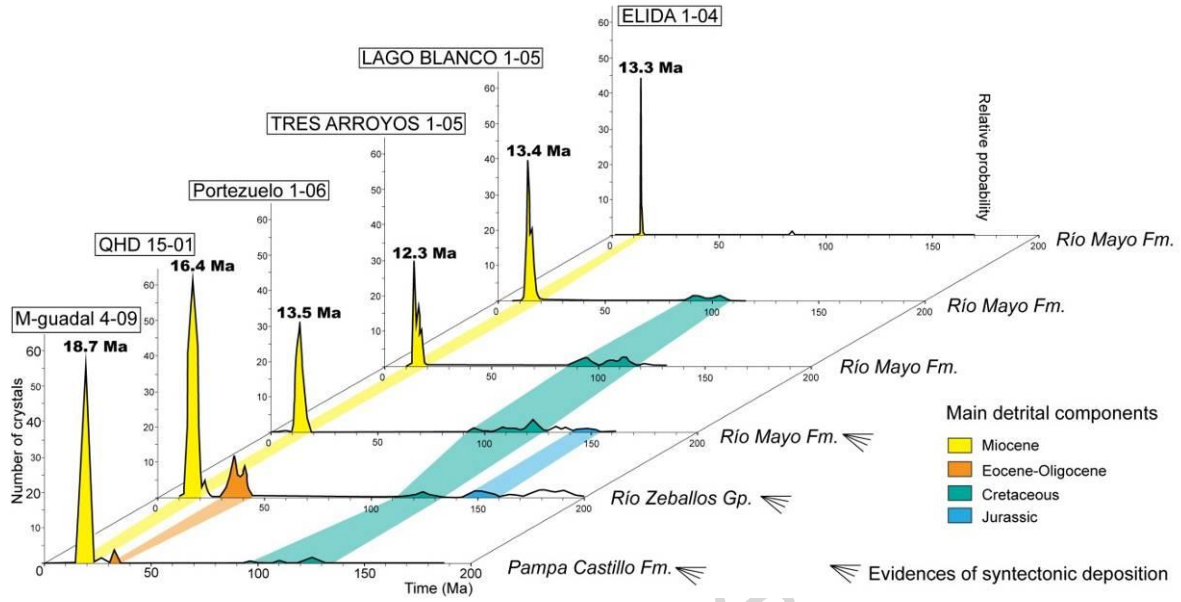
Figure 5. *U-Pb maximum depositional age determinations on Meseta Guadal, Jeinemeni, Meseta Guenguell and Meseta Chalía areas (Río Mayo and Chalía formations) (see Figure 2 for location). U-Pb ages of the Pampa Castillo Formation in the Guadal-Cosmelli syncline have yielded a maximum age of 18.7 Ma, while the Jeinemeni strata of the Río Zeballos Group indicate a maximum age of 16.6 Ma and the Río Mayo Formation in the Portezuelo region 13.5 Ma. Note a peak around ~125 Ma and another around 150-160 Ma in the lower Miocene continental deposits corresponding to a recycled tuff of the Pampa Castillo Formation whose maximum age is 18.7 Ma that continue in the 16.6 and 13.5 Ma deposits, indicating an Andean provenance. Note also a recycled population around 29-20 Ma in the lower terms widely exposed in volcanic units of the Chilean Andean slope. For the Meseta Chalía surroundings, coarse sediments of the Pedregoso Formation have been dated through a basal tuff that yielded 13.3 Ma (U-Pb). To the south, an upper section crowning the meseta next to Estancia Tres Arroyos was dated, where surge and recycled deposits yielded 12.3 Ma (U-Pb) (note the recycling of 14.8 Ma populations in the basal terms, indicative of the cannibalization of the western depocenters with an age equivalent to the sediments dated in the Río Cisnes area). To the east near Lago Blanco, sandstones of the Río Mayo Formation have yielded a maximum age of 13.4 Ma, also showing the recicling of an older population with 15.4 Ma age.*

28

6.2 Field data

6.2.1 New U-Pb and structural data in Meseta Guadal area

We dated a reworked tuff bed (sample MGuadal 4.09) located 10 meters above the basal contact of the Pampa Castillo Formation at Meseta Guadal and obtained a U-Pb age of 18.7 Ma (Burdigalian) and two additional age peaks of 28-32 Ma (Oligocene) and of 98-130 Ma (Cretaceous) (Figures 4 and 5). Suárez et al. (2015) obtained a similar U-Pb (SHRIMP) age of ~18 Ma from a tuff of the same unit. Even though we did not observed direct evidence of growth strata in Pampa Castillo Formation during our field work, internal unconformities and variable thickness in strata of this unit associated with contractional structures are identified in satellite images (Figure 6).
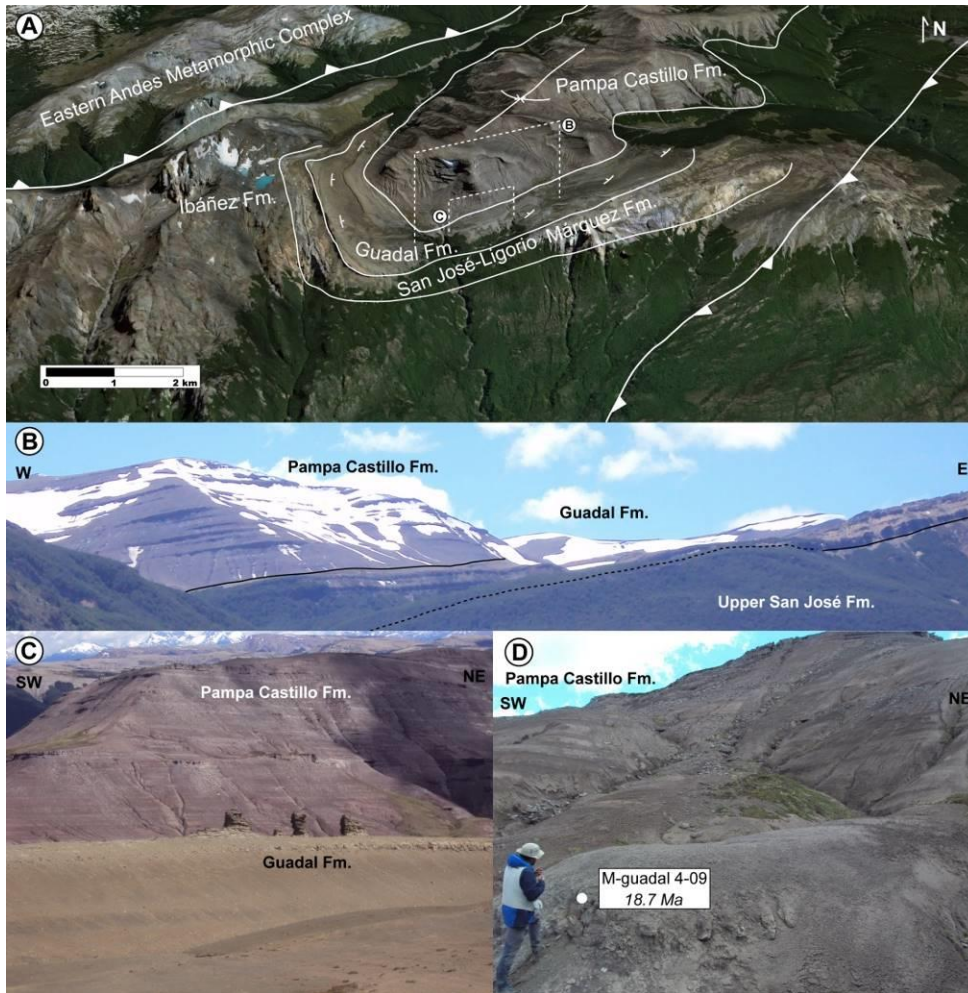
Figure 6. *Continental strata of the Pampa Castillo Formation overlying marine strata of the Guadal Formation at Pampa Castillo, in the southern part of the Meseta Guadal syncline (see location in a map view in Figure 2). A) Digital elevation model constructed with TM image draped on top of it for an oblique view of the Meseta Guadal syncline. B and C) Details of internal unconformities and variable thickness of strata of the Pampa Castillo Formation. D) Picture showing concordant relations between the fluvial strata of the Eocene San José Formation, the marine strata of the upper Oligocene-lower Miocene Guadal Formation, and the fluvial strata of the lower Miocene Pampa Castillo Formation. E) Detail of the gradual contact between Guadal and Pampa Castillo formations. F) Basal part of the Pampa Castillo Formation where a U-Pb age of 18.7 Ma (sample MGuadal 4-09) was obtained (see Figures 4 and 5).*

6.2.2 New U-Pb and structural data in the Jeinemeni area

South of Chile Chico, at ~46°40'S, a reverse fault referred to as the Jeinemeni Fault (De la Cruz and Suárez, 2008) overthrusts Mesozoic and Cenozoic strata over the Río Zeballos Group (Figure 2). Near this fault trace, we observed a succession of near vertical Mesozoic and Cenozoic strata that, from east to west correspond to the Jurassic Ibáñez, Lower Cretaceous Toqui, and Cenozoic Ligorio Márquez and Guadal formations. West of the fault, strata of the Río Zeballos Group present a predominantly subhorizontal orientation, although they show more deformation near the fault trace, including folds and reverse faults of small scale. At the confluence between the Quebrada Honda and the Río Jeinemeni, we observed small scale thrusts that exhibit growth strata fans and internal unconformities at their backlimbs that are overlain by undeformed horizontal strata (Figure 7).

The deformed strata were assigned to the Lower Galera Formation and the overlying horizontal strata to the upper Galera Formation by Ray (1996). According to the description of Escosteguy et al. (2002, 2003), they can be assigned to the Río Jeinemeni and Cerro Boleadoras formations respectively. We dated (U-Pb method) a sandstone (Sample QDH 15-1) from an outcrop at the confluence between the Quebrada Chica and the Quebrada Honda that was assigned to the Upper Galera Formation by Ray (1996) (the Cerro Boleadoras Formation), obtaining a maximum age of 16.4 Ma (Figures 4 and 5). Other minor zircon populations are represented by an Oligocene age peak (27-33 Ma) and a Cretaceous component (84-128 Ma).
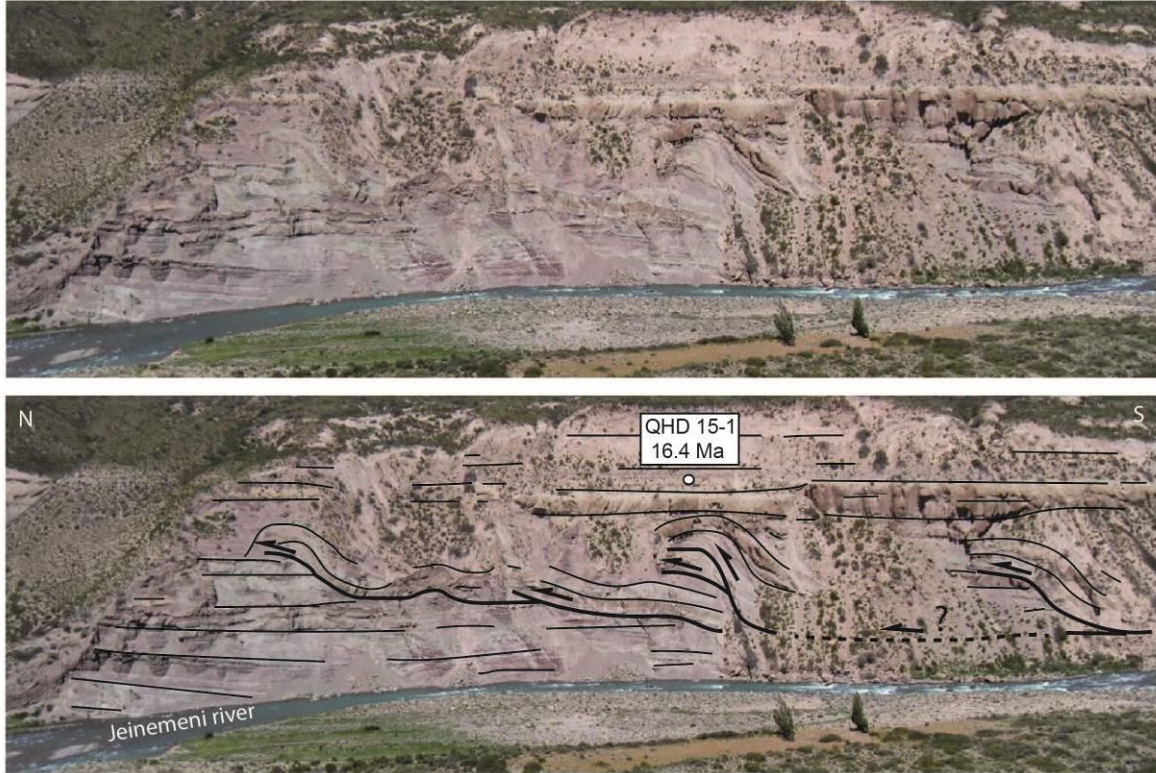
Figure 7. *Internal angular unconformity that separates the Río Jeinemeni and Cerro Boleadoras formations and growth strata associated with contractional structures in the Río Zeballos Group associated with minor-scale contractional structures in the Jeinemeni valley, near the confluence of this river with the Quebrada Honda creek (see location in a map view in Figure 2). The obtained 16.4 Ma (maximum age; U-Pb) age is above the unconformity in the Cerro Boleadoras Formation.*

6.2.3 Identification of growth strata in the Alto Río Cisnes area

In the Nacientes de Río Cisnes (Figures 2 and 8), sedimentary strata of the Río Frías Formation are overthrust by Cretaceous volcanic sections of the Divisadero Group. At the footwall, a series of backthrusts deform the southern border of the Neogene depocenter. In

the deformed sector (Figure 8), growth strata, wedge geometries and onlap relations indicate internal deformation during deposition of these sequences.

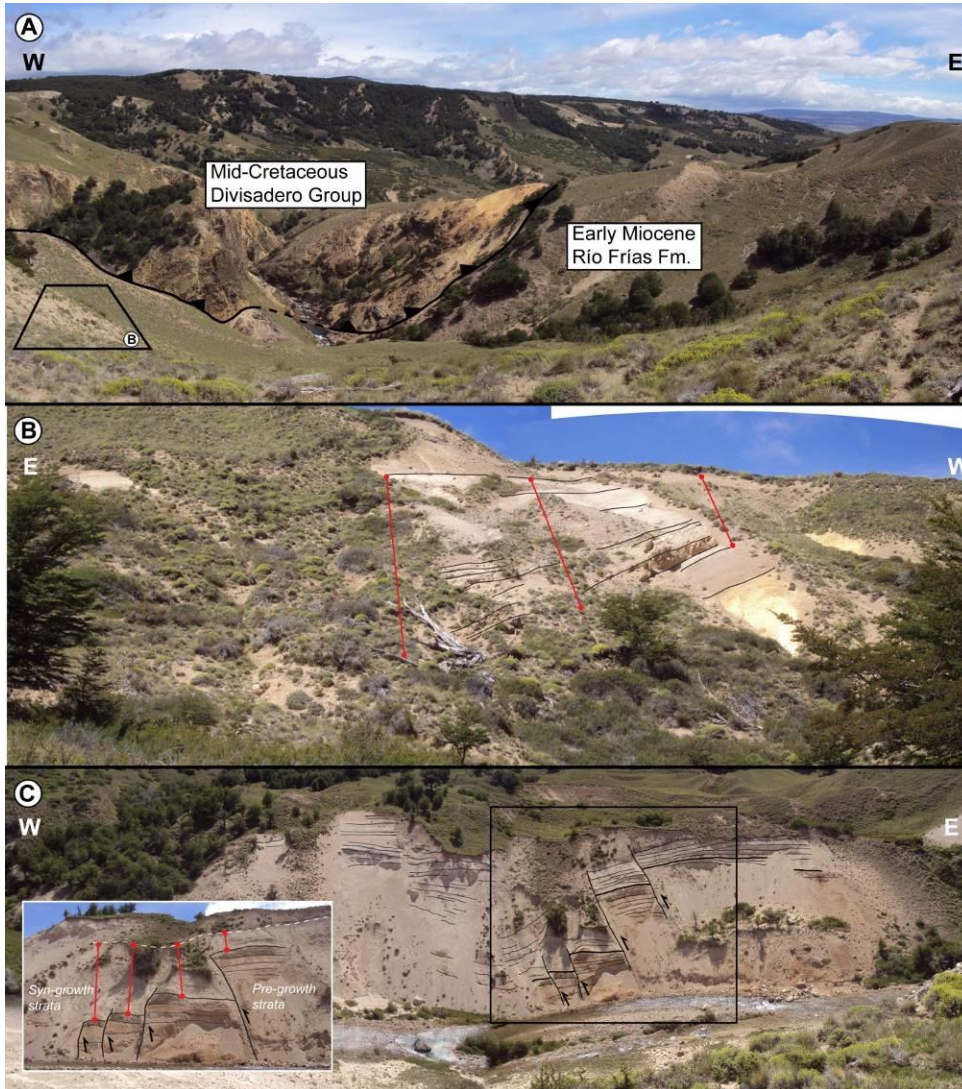**Figure 8.** *Growth strata of the Río Frías Formation dated by Encinas et al. (2016) at 15.8 Ma at the footwall of a thrust that overlies Lower Cretaceous rocks of the Divisadero Formation over Cenozoic strata at the Nacientes de Río Cisnes locality. A) Thrust that uplifts Cretaceous strata on top of the Río Frías Formation. B) Detail of growth strata in the footwall of the thrust shown in A. C) Variable*

thickness of synorogenic strata wedges towards syngenetic contractional structures forming a fan of backthrusts (see location in Figure 2).

6.3.4 New U-Pb data in the Meseta de Chalía area

We dated a reworked tuff (sample ELIDA 1.04) interbedded with conglomerates from the basal part of the Pedregoso Formation at the same section and obtained an age of 13.3 Ma (Figures 4, 5, and 9), with only two older zircon grains of 87 and 170 Ma.

South of this locality, at the Estancia Tres Arroyos in the Meseta Chalía, we observed a succession of tuffs with minor conglomerates included in the Río Mayo Formation by Dal Molín and Franchi (1996) (Figure 9D). These are interpreted as surges and reworked pyroclastic materials with water escape features. The base and the top of these strata are covered but we observed a succesion of gravels at the top of the hill where they crop out that were mapped by Dal Molin et al. (1998) and Franchi et al. 1995) as corresponding to the Chalía Formation. We dated a lithic lapilli reworked tuff (sample Tres Arroyos 1.05) of the Estancia Tres Arroyos volcaniclastic succession and obtained an age of 12.3 Ma (Figures 4, 5 and 9) and subordinate peaks of ~15 Ma (middle Miocene) and 88-111 Ma (Cretaceous).

Near Lago Blanco (Figure 2), we observed a succession of sandstones and silstones corresponding to relatively distal fluvial systems (Figure 9D), also included in the Río Mayo Formation by Franchi et al. (1995). A sandstone of this succession (sample Lago Blanco 1.05) was dated by the U-Pb method obtaining a maximum age of 13.7 Ma (Figures 4 and 5) and subordinate peaks of ~15 Ma (middle Miocene) and ~92-107 Ma (Cretaceous).
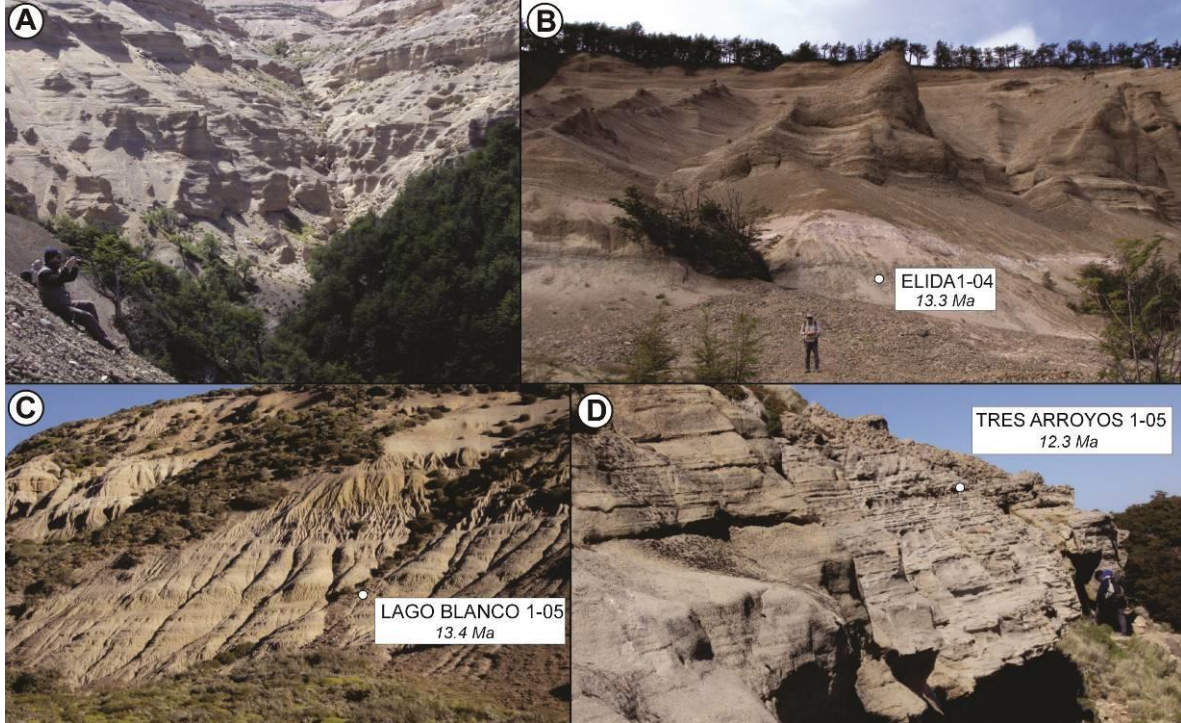
34

Figure 9. *A) Fluvial conglomerates of the Pedregoso Formation at Meseta Chalía. B) Tuff bed overlain by conglomerates of the Pedregoso Formation. The tuff yielded an U-Pb age of 13.4 Ma (sample Elida 1.04) C) Tabular sandstones and siltstones of the Río Mayo Formation at the Lago Blanco locality. Sample Lago Blanco 1.05 yielded a maximum age of 13.4 Ma. D) Surge deposits and reworked tuffs of the Río Mayo Formation at the Estancia Tres Arroyos (Meseta Chalía). Sample Tres Arroyos 1.05 yielded an age of 12.3 Ma (see location in Figure 2).*

6.2.5 New U-Pb and structural data in the Meseta de Guenguell area

In western Meseta Guenguell, growth structures in a succesion composed of ammalgamated ignimbrites and reworked pyroclastic deposits crop out in the footwall of a west-vergent thrust that uplifts Cretaceous volcanic rocks of the Divisadero Group (Figures 2 and 10A -

B). U-Pb dating in zircons of a reworked tuff of this succession (sample Portezuelo 1.06) have yielded a maximum age of 13.5 Ma (Figures 4, 5 and 10) and a subordinate population of 94-148 Ma (Upper Jurassic to Cretaceous).

Twelve and a half km to the north, along the western bank of the Río Simpson, we observerd strata of the El Portezuelo Formation with onlap relations in the frontal limb of an anticline with a west-vergence (Figure 10C).
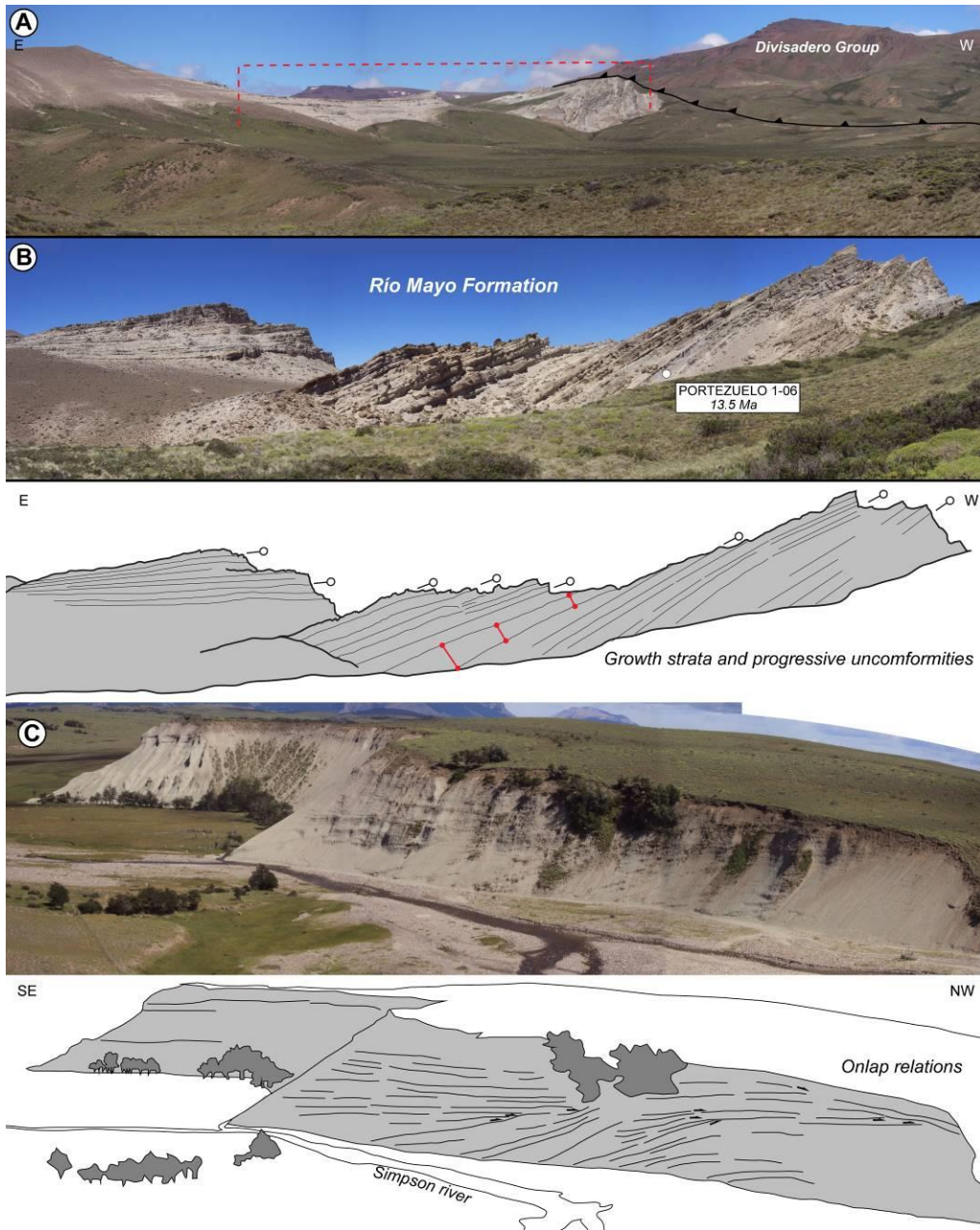
Figure 10. *A) Ignimbrites and pyroclastic deposits of the El Portezuelo Formation dated at 13.5 Ma*

(sample Portezuelo 1.06; see Figures 4 and 5) at Cerro El Portezuelo. These growth strata are

developed at the footwall of a thrust that uplifts Cretaceous volcanic rocks of the Divisadero Group

in the eastern Main Andes. B) Interpretation of growth strata and location of sampled unit. C) Frontal

limb of a west-vergent anticline in the western flank of the Meseta Guenguell associated with growth

structures in the El Portezuelo Formation strata at the Río Simpson (view to the SW). Arrows and ticks indicate onlap / offlap relations and variable lateral thickness of strata respectivelly (see location in Figure 2).

7. DISCUSSION

7.1 Age constraints of Neogene synorogenic deposits

Our data constrain early-middle Miocene synorogenic continental deposition in the study area to the 18.7-12.3 Ma interval (Figures 4 and 5). The oldest age of 18.7 Ma corresponds to a reworked tuff dated by the U-Pb method at the base of the Pampa Castillo Formation at Meseta Guadal. This age is similar to those of ~19-18 Ma determined for the base of correlative continental deposits in the western extra-Andean region of Patagonia between 49-51°S (see Cuitiño et al., 2016); it is coincident or slightly older than the 18.3 and 17.7 Ma ages assigned to marine strata of the Cerro Plataforma and La Cascada formations (maximum ages from U-Pb in detrital zircons) that crop out in the eastern and western flanks respectively of the North Patagonian Andes at ~43°S (Orts et al., 2012; Encinas et al., 2014); although it is older than the age of 17.4 Ma marine "Patagonian" strata of the Sierra San Bernardo (~46°S) in the extra-Andean region (Encinas et al., 2016; Gianni et al., 2017); and older than the 19.6–15.3 Ma marine deposits of the Chenque Formation (Cuitiño et al., 2015) and the 22.1–17.9 Ma Monte León Formation (Parras et al, 2012) both in the Atlantic coast of Argentina (Figure 3). These data imply that early Miocene continental and marine deposition in Patagonia were partially contemporaneous and that the marine deposits of the

"Patagoniense" gradually withdrew eastwards as the synorogenic continental deposits prograded to the foreland region.

The youngest age of 12.3 Ma for the continental deposits at the study area corresponds to a reworked tuff from the upper part of the Río Mayo Formation in Estancia Tres Arroyos, at Meseta Chalía. The age is approximately coincident with that of De Iuliis et al. (2008) of 11.8 Ma (Ar-Ar method) from a tuff of the same unit at Meseta Guenguell and those of 12.3 and 12.1 Ma from likely correlative strata in the adjacent area of the Río Oscuro in Chile (Rivas et al., 2015). The new 12.3 Ma age is almost coincident with the 12.4 Ma age for the base of the Meseta Lago Buenos Aires Formation (Guivel et al., 2006) that overlies the strata of the Río Zeballos Group that put an end to the synorogenic continental deposition in Patagonia (Figure 3). There are no younger continental deposits in the Andean Cordillera nor in the extra-Andean region at these latitudes with the exception of upper Miocene-Pleistocene glacial and fluvioglacial deposits (Mercer and Sutter, 1982; Lagabrielle et al., 2007) and to the Chalía Formation gravels, which are probably related as well to the (latest Miocene) Plio-Pleistocene glaciations that occurred in this area (Lagabrielle et al., 2004). These data indicate that Neogene contractional deformation and synorogenic deposition of fluvial and volcanoclastic strata in this area were restricted to a very short interval of approximately 6.5 My.

The continental deposits in the study area present either a coarsening-upward or a coarsening upward followed by a fining-upward tendency. The only exception is the 131 m thick Río Frías Formation in the Alto Río Cisnes area (Figure 8) that does not present a clear grain-size

variation, although this could be due to erosion of the upper part of this unit as it presents a marked disconformity with an overlying conglomeratic succession.

At Meseta Guadal, the only available radiometric ages for the Pampa Castillo Formation are two U-Pb dates of 18.7 Ma (Figure 6; this work) and ~18 Ma (Suárez et al., 2015) obtained from reworked tuffs of the base of the formation, which implies that the upper and coarser-grained part of this unit is younger.

At the Río Jeinemeni area, the Río Zeballos Group shows a coarsening upward succession where the thin bedded siltstones and sandstones of the Río Jenemeni Formation are overlain by the sandy deposits of the Cerro Boleadoras Formation and these by the conglomerates and sandstones of the Río Correntoso Formation (Escosteguy et al., 2003). We obtained a maximum age of 16.4 Ma (Figure 7; U-Pb in detrital zircons) from a succession that we assigned to the Cerro Boleadoras Formation. Thus, the conglomeratic strata of the Río Correntoso Formation that overlie the latter unit are younger than 16.4 Ma and probably in the range of, or older than the ~16 and 14 Ma interval assigned to the Zeballos Volcanic Sequence in the top of the Río Zeballos Group (Espinoza et al., 2010; Boutonnet et al., 2010).

 The Meseta Guenguell area shows a coarsening-upward, then fining-upward Miocene succession composed of reworked tuff, siltstone and sandstone at the base (the Unit 2 of Rivas et al., 2015) that are overlain by sandstones and conglomerates of the El Portezuelo Formation, which pass upward to the finer-grained succession of tuff, sandstone, siltstone, and conglomerate of the Río Mayo Formation (Escosteguy et al., 2002, 2003). The age of the

lower tuff unit of the Meseta Guenguell succession has been assigned to the lower-middle Miocene based on preliminary studies of vertebrate fossils (Rivas et al., 2015). Several radiometric dates are available for the overlying El Portezuelo Formation. This unit was assigned to the middle Miocene (Ar-Ar dating) by Escosteguy et al. (2003). We dated in 13.7 Ma (U-Pb) growth strata in a succession of ignimbrites and reworked tuffs from Cerro El Portezuelo (Figure 10), while Rivas et al. (2015) dated fluvial sandstones in Chile obtaining a similar age of 12.3 Ma with the same method. Yet the presence of Mayoan vertebrate fossils in these strata indicates that they could correspond to the younger Río Mayo Formation. The only available radiometric dating from the latter unit in this area is that of 11.8 Ma (Ar-Ar) from a tuff (De Iuliis et al., 2008).

At Meseta Chalía the coarse-grained conglomeratic deposits of the Pedregoso Formation overlie an unnamed Eocene tuff unit (Gianni et al., 2017) and underlie a finer-grained succession of tuff, tuffaceous siltstone, sandstone, and conglomerate of the Río Mayo Formation. In accordance with Lagabrielle et al. (2004) and contrary to Dal Molin and Franchi (1996), we consider that part of the gravels assigned to the Chalía Formation are probably related to the Plio-Pleistocene glaciations that afected this area and are not entirely part of the synorogenic sequence but this notion needs confirmation. We dated a tuff from the basal part of the Pedregoso Formation with the U-Pb method and obtained an age of 13.3 Ma. A tuff from the upper part of the Río Mayo Formation dated with the same method yielded an age of 12.3 Ma in Estancia Tres Arroyos (Figures 9B and D).

Even though the tectonosedimentary evolution differs depending on the area, these results indicate that after the retirement of the Patagonian sea, fine-grained fluvial and volcanoclastic synorogenic deposits started to accumulate around 18.7 Ma. The uplift of the Andes led to deposition of progresively coarser-grained sediment in higher energy fluvial environments. In the Meseta Chalía area, the 250 to 500 m thick cobble conglomerates and minor sandstones of the Pedregoso and Galera formations were deposited between 13.3 and 12.3 Ma (the latter is a minimum age since it corresponds to the upper part of the Río Mayo Formation). The deposition of this thick conglomeradic sucession in less than 1 My likely reflects a rapid uplift. Since the finer-grained deposits of the Río Mayo Formation overlie the Pedregoso Formation, it is probable that a deceleration in mountain growth activity occurred during the deposition of this unit (~12.3 Ma).

7.2 Neogene lateral growth of the Central Patagonian Main Cordillera (~45-47°S)

Our data and those published in previous works permit to refine the sequence of Neogene uplift of the Central Patagonian Andes between ~45-47°S. Paleocurrent analysis indicates a predominantly eastward direction of sediment transport for the different Miocene units deposited in this area, which dictates that the source areas had to be located to the west of the different sub-basins (Skarmeta, 1976; Ray, 1996; De la Cruz and Suárez, 2006; Rivas et al., 2015). In particular, the Miocene fluvial deposits of the Pampa Castillo Formation at the Meseta Guadal syncline are the only units in the entire Patagonian Andes that are preserved in the axial part of the Main Andean Cordillera. The 18.7 Ma age of the basal part of this unit is aproximately coincident with those of equivalent deposits assigned to the Santa Cruz

Formation in the western part of the extra-Andean region of Patagonia and ~1 My older than those of the same unit in the Atlantic coastal localities (see Cuitiño et al., 2016 and references therein). Upper Oligocene (?) to Pliocene marine strata are exposed in the Golfo the Penas to the west (Forsythe and Nelson, 1985; Covacevich and Frassinetti, 1986; Stott and Web, 1989; Encinas et al., 2015), therefore the narrow mountain belt (~130 km wide) located between the Taitao Peninsula and Meseta Guadal (Figure 2) must have started to uplift around 18.7 Ma. As a consequence, fluvial deposits derived from its erosion accumulated at Meseta Guadal and the western part of the extra-Andean region and ~1 My later reached the Atlantic coast of Argentina. Analysis of provenance based on detrital zircons for our MGuadal 4.09 sample (a reworked tuff from the base of the Pampa Castillo Formation) shows the presence of 18.7, 28-32, 98-130, 303 Ma and older zircon peaks (Figure 5). The young and more abundant peak of 18.7 Ma likely reflects the explosive volcanism contemporaneous with fluvial sedimentation. The 28-32 Ma peak could be derived from Eocene-Oligocene rocks that crop out in the area (Figures 2 and 5). The 98-130 Ma Cretaceous group could correspond to plutonic rocks of the Patagonian Batholith to the west or to volcanic and sedimentary rocks located principally to the east. The 303 Ma zircons could correspond to Carboniferous metamorphic rocks as part of the Eastern Metamorhic Series that crop out in the Main Cordillera (Figure 2). Suárez et al. (2015) analyzed detrital zircon samples from the Pampa Castillo Formation and obtained approximately similar age ranges and peaks of 1984-378, 127-124, 107-96, and 34-18 Ma. They also noticed that one of their samples yielded almost exclusively Precambrian to Paleozoic detrital zircons, which could indicate exhumation of the basement metamorphic rocks from the Main Cordillera and adjacent foreland at the time of this sample deposition.

To the east, the U-Pb age of 16.4 Ma of a sandstone bed that we assigned to the Cerro Boleadoras Formation and the presence of deformed synorogenic strata of the underlying Río Jeinemeni Formation in the Río Jeinemeni area constrain contractional deformation time at this locality. However, this data must be taken with caution because it constitutes a maximum age detrital zircons. Thus, it is not clear whether deformation in this area is coeval or younger than that of the Meseta Guadal area. Importantly, the Río Zeballos Group does not crop out in the Meseta Chile Chico area, west of the Jeinemeni Fault, where the younger Basaltos Superiores de la Meseta Chile Chico Formation directly overlie the upper Miocene marine strata of the Guadal Formation (De la Cruz and Suárez, 2008). In contrast, the equivalent Meseta Lago Buenos Aires Formation overlies the Río Zeballos Group east of the fault (Figure 3). This indicates that the uplift of the Meseta Chile Chico started after deposition of the Guadal Formation. Analysis of provenance based on detrital zircons for our QHD 15-1 sample indicates the presence of 16.4, 27-33, 84-128, and 167 Ma zircon peaks (Figure 5). The youngest group probably corresponds to explosive volcanism contemporaneous with sedimentation. The 27-33 Ma group probably derives from Eocene-Oligocene volcanic rocks. The 84-128 Ma group likely derives from Cretaceous volcanic and sedimentary rocks.

The presence of growth strata in the Río Frías Formation at the Alto Río Cisnes area indicates their synorogenic origin. Some discrepancy exists in the age of this unit (see above) but the U-Pb age of 15.8 Ma recently obtained by Encinas et al. (2016) is in accordance with paleontologic studies by Bostelmann et al. (2012a, b) who proposed that the Río Frías fauna

is similar to the Colloncuran fauna of Argentina dated in 15.7 Ma by Flynn and Swisher (1995) (Figure 3).

The U-Pb age of 13.5 Ma that we obtained from growth strata at Cerro El Portezuelo (sample Portezuelo 1.06) indicates that the uplift of this area occurred after the uplift of the Meseta Guadal, and Río Jeinemeni, and Nacientes de Río Cisnes areas. This sample also contains a group of 94-148 Ma zircons that were likely derived from Jurassic-Cretaceous volcano-sedimentary rocks from the eastern Andean Cordillera to the west. The thick succession of cobble conglomerates of the Pedregoso Formation, the basal part of which was dated at 13.3 Ma (sample Elida 1.04), was likely deposited as a consequence of the same orogenic pulse. This sample also contains Cretaceous and Jurassic zircons (87 and 170 Ma) that likely derive from the Andean Cordillera to the west (De la Cruz et al., 2003). After an important and rapid pulse of uplift that gave way to this thick conglomeratic succession, contractional deformation and uplift likely dimished sometime before 12.3 Ma as indicated by the accumulation of the finer-grained deposits of the Río Mayo Formation. Two samples from this unit yielded ages of 12.3 Ma (Tres Arroyos 1.05) and 13.4 Ma (Lago Blanco 1.05) the latter being a maximum depositional age. Both samples also contain Cretaceous zircon groups (88-111 and 92-107 Ma) that were derived from the Andean Cordillera to the west and middle Miocene (15 Ma) that probably derive from canibalized synorogenic strata.

Then, Neogene uplift of the Patagonian Andes started at 18.7 Ma giving way to deposition of synorogenic fluvial strata that initially extended between the Meseta Guadal and the western part of the extra-Andean region (Figure 11). Progressive uplift of the Andes

45

permitted these deposits to reach the Atlantic coast of Argentina ~1 My later. Initial uplift was probably simultaneous to slightly diachronous in the area located bewteen the Península de Taitao in the Pacific coast and Meseta Guadal and in the Meseta Chile Chico and Naciente de Río Cisnes (18.7-16.4 Ma). This uplift stage reached the San Bernardo system (broken-foreland system) in the foreland area, where Paredes et al. (2006) described growth strata in marine deposits of the "Patagoniano" and Gianni et al. (2017) dated synorogenic facies in 17.7 Ma associated with its eastern-thrust front in the same unit (Figure 11), implying a broad orogenic configuration at this time. Similarly, Bilmes et al. (2013) described synorogenic sedimentation of 15 Ma for the northern section of this broken-foreland system indicating that contraction reached an easternmost position by 17.7-15 Ma (Figure 12).

Subsequently, the deformation front retracted to the west and reached the eastern limit of the Main Cordillera at around 13.5-13.3 Ma (Figures 11 and 12). Contractional deformation and uplift likely dimished sometime before 12.3 Ma as indicated by the accumulation of the finer-grained deposits of the Río Mayo Formation. Finally, contractional deformation in this area finished at ~12 Ma when upper middle Miocene to Pliocene plateau basalts were emplaced in an extensional regime as pointed out by Lagabrielle et al. (2007).

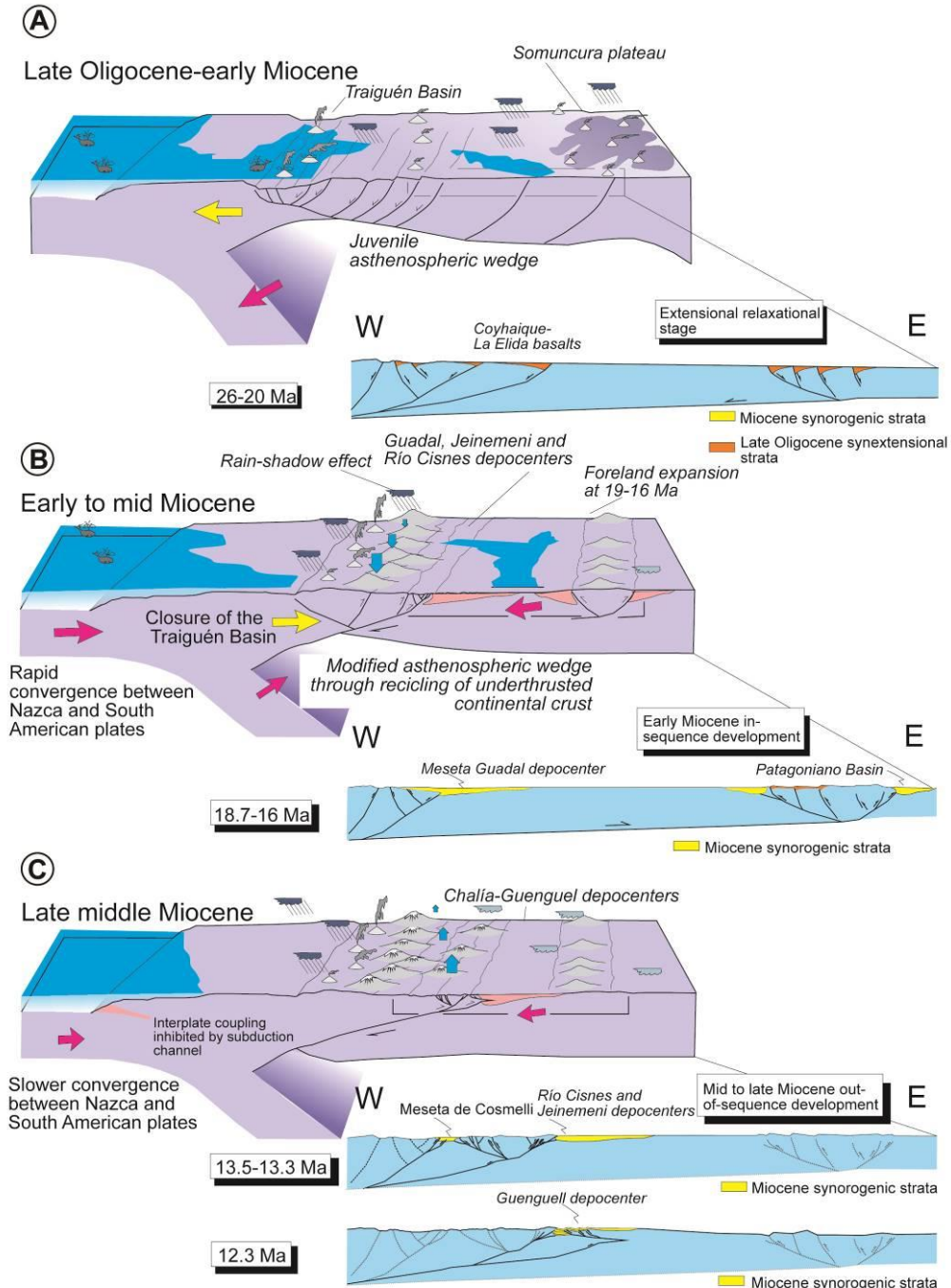**Figure 11.**

Schematic cartoon and structural sections showing the evolution of the Central Patagonian

Andes (structural and geological data taken from De La Cruz et al. (2003a, b), De La Cruz and

Suárez (2008), Suárez et al. (2007), and data of this work): a) After an Eocene contractional stage

(Gianni et al., 2017), an extensional regime in late Oligocene-early Miocene times (~28-20

Ma) was associated with intra-arc volcano-sedimentary-extensional basins (Morata et al., 2005; Encinas et al., 2016; Gianni et al., 2017) and a transgression of Pacific and Atlantic origin (Orts et al., 2012; Bechis et al., 2014; Encinas et al., 2016, 2017). b) The initial uplift of the Andes is characterized by synorogenic continental strata of the Pampa Castillo Formation (18.7 Ma U-Pb). In this stage, the uplift of the San Bernardo system in the foreland area is associated with the synorogenic Patagoniano Basin (17.7 Ma) where marine sedimentation continued during the regression of the Patagonian sea (Paredes et al., 2013; Gianni et al., 2017). c) Out-of-sequence contraction, cannibalization of previous depocenters, and new synorogenic sedimentation in the Meseta Chalía-Guenguell depocenters of ~13.5-12.3 Ma. See location of section in Figure 2.
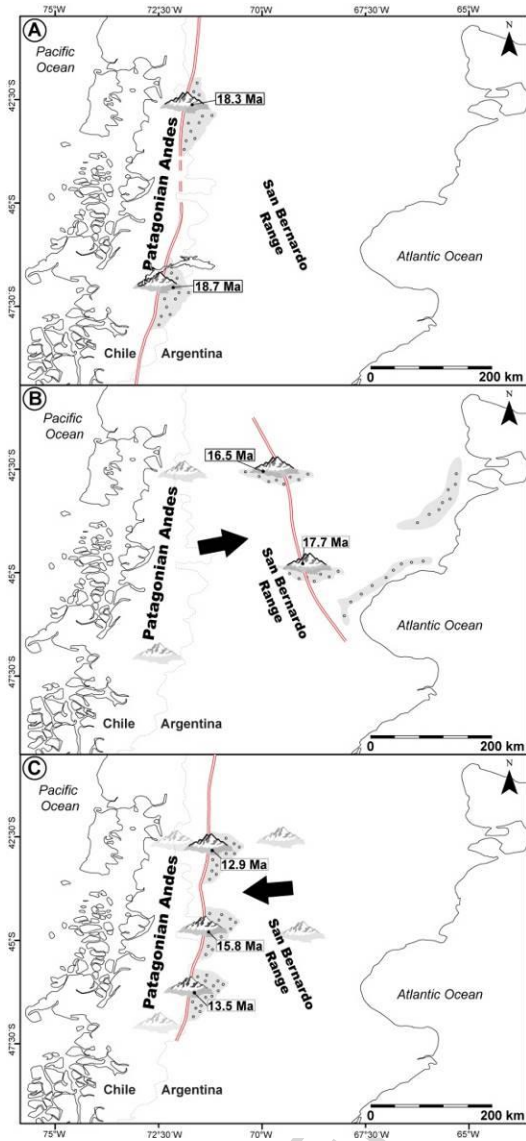
Figure 12. *Deformational fronts in the Patagonian Andes between 19 and 12 Ma based on the position of synorogenic strata. Age determinations are from Paredes et al., (2006), Orts et al. (2012), Bilmes et al. (2013), Ramos et al. (2015), Gianni et al. (2017) and this work. A) Between 18.7 and 16 Ma a wide orogenic configuration spreads through Patagonia with synorogenic depocenters associated with the Main Cordillera in the west and B) the broken-foreland system in the east. C) After 13.5 Ma and until 12.3 Ma, a retraction of the orogenic activity occurs growing in an out-of-sequence order the Main Cordillera.*

7.3 Comparison with the progression of Neogene deformation in the northernmost

Patagonian Andes

Recent works focused on synorogenic strata in the North Patagonian Andes some 350 km

north of the study area (~41-43°S), provided a framework to analyze and compare how

Neogene deformation progressed through time in northern Patagonia (Figure 12).

The oldest synorogenic sedimentation in the North Patagonian region accumulated next to

the axial Main Andes in the Cerro Plataforma depocenter (Fig. 2) (Orts et al. 2012; Encinas

et al., 2016). In this area over the Argentinean side, 18.3 Ma shallow-marine deposits show

progressive unconformities associated with a frontal syncline, which indicates synorogenic

deposition related to the uplift of the North Patagonian Andes (Figure 12) (Orts et al. 2012).

U-Pb ages in detrital zircons indicate that the axial Andean sector was constructed in the lapse

~18-17 Ma (Orts et al. 2012). After this, a rapid propagation of the orogenic wedge occurred,

whose frontal easternmost sector associated with growth structures in the Gastre sector dated

at 14.8 Ma (Ar-Ar; Bilmes et al. 2013) over the western edge of the North Patagonian Massif

corresponding to an eastern broken foreland (Figure 12).

Maximum depositional ages based on U-Pb analysis of detrital zircons associated with

sedimentary sequences of the Ñirihuau and Collón Curá formations with progressive

unconformities in the eastern flank of the El Maitén range have yielded 13.5-11.3 Ma,

indicating that this sector, located in the western broken foreland (Precordillera) grew in an

out-of-sequence order respect to the frontal sectors of the Gastre region (Ramos et al. 2011, 2015). Thus, a 1,600 m thick synorogenic depocenter developed as a consequence of the exhumation of intermediate sectors of the North Patagonian fold and thrust belt, leaving to the east a broad sector structured in the previous early Miocene stages (Figure 12).

This scheme keeps strong similarities with data presented in this work, where initial synorogenic sedimentation, yielding an age of 18.7 Ma, started with deposition of the fluvial Pampa Castillo Formation in the Meseta Guadal syncline. As noted before, fluvial and marine sedimentation coexisted in different areas of the Andean Cordillera and the foreland during the initial stages of Andean uplift and prior to the definitive regression of the Patagonian sea (Encinas et al., 2017). This explains coeval deposition of marine and continental sediments in the the Cerro Plataforma and Meseta Guadal respectively around ~18.5 Ma. This implies that by 19-18 Ma only the present western and axial Andes were part of the orogenic wedge and that all the eastern structures are consequently younger. After this initial foreland marine and continental stage, deformation migrated at 17.7-15 Ma to the east to the San Bernardo Precordillera, where marine conditions had prevailed (Paredes et al., 2006; Gianni et al., 2017). Finally, contractional deformation returned to the western sector as out-of-sequence structures that affected and redeformed the orogenic wedge in the eastern Main Cordillera region next to Cohiayque and Balmaceda regions at 13.5-12.3 Ma (Figure 12).

7.4 The role of the collision of the Chilean mid-ocean spreading ridge in the tectonic evolution of the Central Patagonian Andes

Our data indicate that Neogene contractional deformation in the Patagonian Andes at ~45-47°S was limited to a short period bewteen 18.7 and 12 Ma. These ages are consistent with apatite FT data that indicate important denudation at the position of the present-day main topograhic divide in the study area at 16-8 Ma (Figure 13) (Thomson et al., 2001; Haschke et al., 2006a) and also agree with stable isotope analysis that shows an important change in δ^{13}C and δ^{18}0 of pedogenic carbonate nodules at 16.5 Ma, interpreted as indicative of ~1 km of rapid uplift (Blisniuk et al., 2005) (Figure 2).
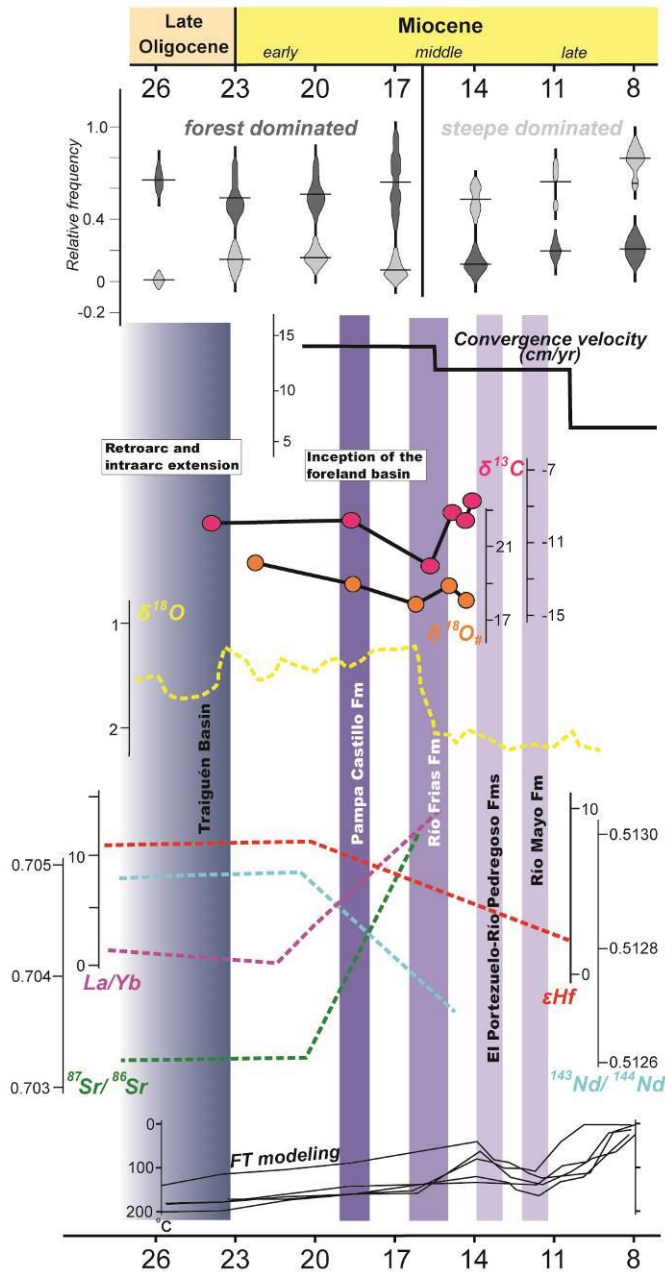
Figure 13. *Comparison of the ages of synorogenic sedimentation described in this work vs. (from above to bottom), pollen changes registered at ~16 Ma in extra-Andean Patagonia (horizontal axes of polygons are proportional to amount of species; for extra details refer to Palazzesi and Barreda, 2012), convergence velocity between Nazca and South American plates through time (Sdrolias and Mueller, 2006), δ13C and δ18O isotopic changes in*

paleosoils (Blisniuk et al., 2005; grey circles), oxigen isotopic changes in sediments of the south Atlantic passive margin (Miller et al., 1987; dashed line), fission track data at 47ºS in the retroarc zone (Haschke et al., 2006a), La/Yb (REE), $^{143}Nd/^{144}Nd$, $^{87}Sr/^{86}Sr$, εHf ratios in contemporaneous arc-magmas interpreted as influenced by crustal thickening and contamination of the asthenospheric wedge (Haschke et al., 2006b; Balgord, 2017) (see Figure 2 for location of these studies).

Flint et al. (1994) and Ramos (2005) attributed rapid mountain uplift and development of a fold and thrust belt in Central and Southern Patagonian Andes to the subduction of the Chilean mid-ocean ridge. In particular, Ramos (2005) proposed that deformation was facilitated by thermal weakening caused by sub-lithospheric heating as a result of ridge subdution. However, contractional deformation in this region pre-dated the latest episodes of ridge collision and the main result of this collision would have been mainly accelerating isotatic uplift and extensional tectonism (e.g., Suárez, 2000; Scalabrino et al., 2010). Plate reconstructions by Cande and Leslie (1986) indicate that initial ridge collision in the southern tip of South America (at ca. 55°S) started at 15–14 Ma and then migrated northwards up to its present position at ca. 46°S. Three segments of the southern Chile Ridge sucessively entered the trench at the southern part of the study area at 6, 3, and 0.3 Ma, while the third is presently subducting to the north of the triple junction point (Cande and Leslie, 1986; Lagabrielle et al., 2007).

Our data indicate that deposition of syntectonic fluvial strata between 18.7 and 12.3 Ma started 4.5 My before subduction of the Chile Ridge at the southern tip of South America and

ended about 6 My before this ridge reached the study area. In addition, the timing for deformation in the study area appears to be aproximately similar to that for the region located to the north at 41-43°S, far away from the Chile Ridge direct influence during the early-middle Miocene (Bilmes et al., 2013; Ramos et al., 2015).

7.5 Paleoecological implications of Neogene uplift of the Patagonian Andes

Fossil evidence is consistent with our data. The occurrence of upper Oligocene-lower Miocene marine deposits in the western, central, and eastern parts of the Patagonian Andes between ~41 and 47°S indicates that the high topography interposed between the Pacific coast and the eastern Andean foothills likely did not exist yet (Encinas et al., 2014; 2017), and that humid winds coming from the Pacific provided sufficient humidity as to allow the development of rainforest taxa in the foreland (Figure 13) (Barreda and Palazzesi, 2007). Contractional deformation and Andean growth at the study area commenced at 18.7 Ma and experienced an important renewal of its denudation at ~13.7-12 Ma. It is likely that the vegetational, and faunal changes caused by a shift to a cooler and more arid climate in the extra-Andean Patagonia around 14 Ma were primarily driven by the uplift of the Andes that attained the suficient height to cause an important orographic rain shadow effect to the east of this mountain belt during this period (Figure 13).

Another point of interest is the contribution of our geochronologic data in the dating of the South American Land Mammal ages (SALMA) (Figure 3). Flynn et al. (2002) and Ugalde et al. (2015) correlated the Pampa Castillo and Pampa Guadal faunas of the Pampa Castillo

Formation with the Santacrucian fauna of Argentina. However, our age of 18.7 Ma for the base of the Pampa Castillo Formation at the homonymous locality suggests that at least the vertebrate fauna in the lower part of this unit could be Notohippidian (Figure 3). Our maximum age of 16.4 Ma for the Cerros Boleadoras Formation strata near the Río Jenemeni could help in future studies on the vertebrate fauna of this unit. In the study area, the Mayoan fauna has been found in strata of the Pedregoso, El Portezuelo, and Río Mayo formations. Franchi et al. (1995) dated a tuff from the Pedregoso Formation by the Ar-Ar method and obtained an age of 12.1 Ma. However, we obtained a U-Pb age of 13.4 Ma. We also obtained an age of 13.5 Ma from a tuff of the correlative El Portezuelo Formation, a maximum 13.4 Ma age from a sandstone strata of the Río Mayo Formation near Lago Blanco and an age of 12.3 Ma from a reworked tuff of the same unit at the Estancia Tres Arroyos. These ages contribute in the determination of the age of the Mayoan fauna and reinforce the notion that it should be placed between the older Collón Curá and Río Frías formations and the younger Arroyo Chasicó Formation.

7.6 Relation between age of synorogenic strata, fission track data, crustal thickening and isotopic changes

Main isotopic changes in sediments, soil formation and magmatism that occurred at the time of synorogenic sedimentation in Central Patagonia, paralleled biota changes, rare earth element (REE) patterns in magmatic rocks and fission track data (Figure 13). At ~16-14 Ma, palinomorphs indicate a passage from forest-dominated to steepe-dominated environments

56

(Figure 13; Palazzesi and Barreda, 2012), when the position of the deformational front, indicated by synorogenic sedimentation, advanced from Meseta Guadal, Río Jeinemeni and Nacientes del Río Cisnes areas to the San Bernardo fold and thrust belt system (Figures 11 and 12). This time coincides with $\delta 18$O isotopic changes in sediments of the South Atlantic passive margin (Figure 13; Miller et al., 1987). Additionally, the time of inception of synorogenic sedimentation at 18-16 Ma is the time of major changes in isotopic composition determined from arc-related rocks from the Patagonian Andes (Figure 13; Haschke et al., 2006b; Balgord, 2017). Higher εNd, εHf and lower εSr isotopic ratios in arc-magmas during pre-orogenic stages indicate low assimilation of low-melting crustal materials and a juvenile asthenospheric source, in accordance with a thin continental lithosphere resulting from an extensional phase (Figure 13). After 18-16 Ma, these ratios changed indicating increased contamination of the asthenospheric wedge with low-melting crustal materials and consequent progressive modification of the arc sources. This can be explained by accretion of a forearc block during the phases of intra-arc Traiguén Basin closure as well as underthrusting of the foreland zone coupled with retro-arc shortening (Folguera et al., 2018) (Figure 11). Fission track data to the south of the study area (Haschke et al., 2006b; Figure 2) indicate that at the time of onset of synorogenic sedimentation, a marked cooling trend establishes that is explained by progressive exhumation coupled with crustal thickening, inferred from La/Yb (REE) ratio (Haschke et al., 2006b).

Finally, these changes could also be associated with changes in plate kinematics (Sdrolias and Muller; 2006; Seton et al., 2012; Somoza and Ghidella, 2012). Deceleration of the convergence rate between Nazca and South American plates since ~16 Ma coincides with

inferred periods of shortening and crustal growth (Figure 13), with a marked drop by 12-11 Ma, when fine grained synorogenic strata deposited. However, potential decoupling of the interplate zone associated with development of the subduction channel since ~16 Ma after conformation of the rain shadow effect, likely constitutes also an important control in tectononic quiescence at these latitudes (Blisniuk et al., 2005).

8. CONCLUSIONS

Our data indicate that, after a period characterized by extensional deformation and a major marine trangression that covered part ot the Central Patagonian Andes during the late Oligocene-early Miocene, a new phase of Andean growth started at 18.7 Ma. The Main Andes deformed and uplifted diachronically from west to east between ~18.7 and 12 Ma. This was achieved through three discrete pulses associated with three generations of synorogenic depocenters: The oldest on the western slope of the Andes around 18.7 Ma with the deposition of the Pampa Castillo Formation; an intermediate one in the east of 16.4-15.5 Ma corresponding to the Jeinemeni strata and Río Frías formations located next to the present drainage divide area, and relatively coeval to synorogenic sedimentation in the Patagonian broken foreland system to the east (17.7-15 Ma); and a younger last pulse located in the eastern Andean front of 13.5-12.3 Ma corresponding to the Pedregoso and Río Mayo formations that registered the recycling of previous synorogenic detrital components. This implies a strong expansion of the orogenic wedge in the 18.7-15 Ma time period in Central Patagonia, followed by a retraction of orogenic activity by 13.5 Ma, and a marked waning

58

by 12 Ma. Contractional deformation in this area finished at ~12 Ma as indicated by undeformed upper middle Miocene alkali flood basalts (Figure 2).

Mechanical weakening of the arc zone, associated with the development of retroarc extensional conditions and emplacement of volcanic plateaux in late Oligocene times could have facilitated and triggered subsequent horizontal collapse and rapid expansion of shortening in the Patagonian crust (Orts et al., 2012, 2017; Echaurren et al., 2016; Gianni et al., 2017). After this rapid expansion of orogenic activity achieved between 18.7 and 15 Ma, out-of-sequence development of the orogenic wedge occurred between 13.5 and 12.2 Ma at the time of plate convergence deceleration (Sdrolias and Muller; 2006; Seton et al., 2012; Somoza and Ghidella, 2012). This could have also been related, as previously proposed by Blisniuk et al. (2015), to a reinforcement of the rain shadow effect and filling of the trench with its lubricating and decoupling effect, although subcritical conditions of the orogenic wedge imposed by erosion of the western sector of the fold and thrust belt and the need of reestablishing the frontal-critical taper cannot be discarded.

Isotopic changes in arc magma composition during this lapse indicate progressive modification of the asthenospheric wedge due to the incorporation of forearc and retroarc low-melting crustal materials during shortening phases. In this line, REE elements and fission track data indicate progressive rock exhumation coupled with moderate crustal thickening during this time (Haschke et al., 2006a, b).

Climatic and biota changes in Central Patagonia evidenced from isotopic and microfossil data seem to be associated with the last pulses of in-sequence Andean construction produced at 18.7-15 Ma and out-of-sequence development. In particular, these data are coherent with paleontogical studies that indicate important changes in the fauna and flora of this region between ~14 and 12 Ma.

Finally, these data indicate that deposition of syntectonic strata between 18.7 and 12.3 Ma started 4.5 My before subduction of the Chile Ridge at the southern tip of South America and ended 6 My before this ridge started to subduct in Central Patagonia.

ACKNOWLEDGMENTS

REFERENCES CITED

Ameghino, F. 1906. Les formations sédimentaires du Crétacé Supérieur et du Tertiaire de Patagonie avec un parallelé entre leurs faunes mammalogiques et celles de l´ancien continent. Anales del Museo Nacional de Buenos Aires (tercera serie) 8: 1-568.

Barreda, V., Palazzesi, L. Patagonian vegetation turnovers during the Paleogene-early Neogene: origin of arid-adapted floras. Bot. Rev. 73, 31–50.

Aragón, E., D'Eramo, F., Castro, A., Pinotti, L., Brunelli, D., Rabbia, O., Rivalenti, G., Varela, R., Spakman, W., Demartis, M., Cavarozzi, C.E., Aguilera, Y.E., Mazzucchelli, M., Ribot, A. 2011. Tectono-magmatic response to major convergence changes in the North Patagonian suprasubduction system, the Paleogene subduction–transcurrent plate margin transition. Tectonophysics 509, 218-237.

Balgord, E. A. 2017. Triassic to Neogene evolution of the south-central Andean arc determined by detrital zircon U-Pb and Hf analysis of Neuquén Basin strata, central Argentina (34-40ºS). Lithosphere. Doi: 10.1130/L546.1.

Barreda, V., Palazzesi, L. 2007. Patagonian vegetation turnovers during the Paleogene-early Neogene: origin of arid-adapted floras. Bot. Rev. 73, 31-50.

Bechis, F., Encinas, A., Concheyro, A., Litvak, V.D., Aguirre-Urreta, B., Ramos, V.A. 2014. New age constraints for the Cenozoic marine transgressions of Northwestern Patagonia, Argentina (41°–43° S): paleogeographic and tectonic implications. J. South Am. Earth Sci. 52, 72–93.

Bellosi, E., Bostelmann, J., Ugalde, R., Alloway, B., Bobe, R., Carrasco, G., Mancuso, A., Buldrini, K. 2014. Ambientes asociados a la fauna Friasense (Mioceno Medio) en Alto río Cisnes (Aysén, Chile), in: XIV Reunión Argentina de Sedimentología. Puerto Madryn, pp. 40-41.

Bilmes, A. 2012. Caracterización estratigráfica, sedimentológica y estructural del sistema de bajos neógenos de Gastre, provincias de Río Negro y de Chubut. PhD thesis (unpublished), Facultad de Ciencias Naturales y Museo, Universidad Nacional de La Plata, La Plata.

Bilmes, A., D'Elia, L., Franzese, J., Veiga, G., Hernández, M. 2013. Miocene block uplift and basin formation in the Patagonian foreland: The Gastre Basin, Argentina. Tectonophysics 601, 98-111.

Blisniuk, P.M., Stern, L.A., Chamberlain, C.P., Idelman, B., Zeitler, K. 2005. Climatic and ecologic changes during Miocene surface uplift in the Southern Patagonian Andes. Earth Planet. Sci. Lett. 230, 125–142.

Bobe, R., Bostelmann, E., Tejedor, M., Carrasco, G., Mancuso, A., Alloway, B., Bellosi, E., Ugalde, R., Buldrini, K. 2015. Primates del Mioceno de Río Cisnes, Patagonia chilena, in: Simposio "Origen y evolución de los primates platirrinos", pp. 36.

Bostelmann, E., Buldrini, K. 2012. Late-Early Miocene fossil mammals of the Pampa Guadal Area, Meseta Cosmelli, Aysén Region, Chilean Patagonia, in: Leppe, M., Aravena,

J.C., Villa-Martínez, R. (Eds), Abriendo ventanas al pasado. III Simposio de Paleontología en Chile. Punta Arenas, pp. 38-41.

Bostelmann, E., Bobe, R., Carrasco, G., Alloway, B.V., Santi-Malnis, P., Mancuso, A., Agüero, B., Alemseged, Z., Godoy, Y. 2012a. The Alto Río Cisnes fossil fauna (Río Frías Formation, early Middle Miocene, Friasian SALMA): a keystone and paradigmatic vertebrate assemblage of the South American fossil record, in: Leppe, M., Aravena, J.C., Villa-Martínez, R. (Eds), Abriendo ventanas al pasado. III Simposio de Paleontología en Chie. Punta Arenas, pp. 46-49.

Bostelmann, E., Le Roux, J. P., Vasquez, A., Gutiérrez, N., Oyarzún, J. L., Carreño, C., Torres, T., Otero, R., Llanos, A., Fanning, C.M., Nielsen, S.N., Hervé, F. 2012b. A revised lithostratigraphy of the Sierra Baguales, Magallanes Basin, in: XIII Congreso Geológico Chileno. Santiago, pp. 3-5.

Boutonnet, E., Arnaud, N., Guivel, C., Lagabrielle, Y., Scalabrino, B., Espinoza, F. 2010. Subduction of the South Chile active spreading ridge: A 17Ma to 3Ma magmatic record in central Patagonia (western edge of Meseta del Lago Buenos Aires, Argentina). J. Volcanol. Geoth. Res. 189, 319-339.

Bourgois, J., Martin, H., Lagabrielle, Y., Le Moigne, J., Jara, J.F. 1996. Subduction erosion related to spreading-ridge subduction: Taitao peninsula (Chile margin triple junction area). Geology 24, 723-726.

Cande, S.C., Leslie, R.B. 1986. Late Cenozoic tectonics of the southern Chile trench. J. Geophys. Res.-Sol. Ea., 91, 471-496.

Carlini, A.A., Scillato-Yané, G.J., Vizcaíno, S.F. 1993. Un Myrmecophagidae (Vermilingua) del Mioceno de Co. Boleadoras, Santa Cruz, Argentina. Ameghiniana 30, 102.

Chang, Z., Vervoort, J.D., McClelland, W.C., Knaack, C. 2006. U-Pb dating of zircon by LA-ICP-MS. Geochem. Geophys. 7, p. 1-14.

Chick, J., Croft, D., Dodson, H., Flynn, J., Wyss, A. 2010. The early Miocene rodent fauna of Pampa Castillo, Chile. Journal of Vertebrate Paleontology, SVP Program and Abstracts Book 2010:71A

Covacevich, V.D., Frassinetti, D. 1986. El género Cancellaria en el Mioceno de Chile con descripción de cuatro especies nuevas (Gastropoda: Cancellariiidae). Rev. Geol. Chile, 28-29.

Cuitiño, J.I., Pimentel, M.M., Ventura Santos, R., Scasso, R.A. 2012. High resolution isotopic ages for the Early Miocene "Patagoniense" transgression in southwest Patagonia: stratigraphic implications. J. South Am. Earth Sci. 38, 110–122.

Cuitiño, J.I., Ventura Santos, R., Alonso Muruaga, P.J. 2015a. Sr-stratigraphy and sedimentary evolution of early Miocene marine foreland deposits in the northern Austral (Magallanes) Basin, Argentina. Andean Geol. 42, 364-385.

Cuitiño, J.I., Scasso, R.A., Ventura Santos, R., Mancini, L.H. 2015b. Sr ages for the Chenque Formation in the Comodoro Rivadavia region (Golfo San Jorge Basin, Argentina): stratigraphic implications. LAJSBA 22, 3-12.

Cuitiño, J.I., Fernicola, J.C., Kohn, M.J., Trayler, R., Naipauer, M., Bargo, M.S., Kay, R.., Vizcaíno, S.F. 2016. U-Pb geochronology of the Santa Cruz Formation (early Miocene) at the Río Bote and Río Santa Cruz (southernmost Patagonia, Argentina): Implications for the correlation of fossil vertebrate localities. J. South Am. Earth Sci. 70, 198-210.

Cuitiño, J.I., Santos, R.V., Scasso, R.A. 2013. Insights into the distribution of shallow-marine to estuarine early Miocene oysters from southwestern Patagonia: Sedimentologic and stable isotope constraints. Palaios 28, 583-598.

Dal Molin, C., Márquez, M., Maisonabe, B. 1998. Hoja Geológica 4571-IV Alto Río Senguerr, provincia del Chubut. SEGEMAR, Escala 1:250000.

Dal Molín, C., Franchi, M. 1996. Reinterpretación estratigráfica de las sedimentitas terciarias del suroeste del Chubut, in: XIII Congreso Geológico Argentino, III Congreso de exploración de Hidrocarburos. Actas 1: 473-478, Buenos Aires.

Dal Molin, C.N., Colombo Piñol, F. 2003. Sedimentación neógena en la Cuenca del Río Zeballos y del Río Jeinemeni (47Q de Latitud Sur). Antepaís patagónico, Argentina. SGE 34, 139-142.

De Iuliis, G., Brandoni, D., Scillato-Yané, G.J. 2008. New remains of Megathericulus patagonicus Ameghino, 1904 (Xenarthra, Megatheriidae): information on primitive features of megatheriines. J. Vertebr. Paleontol. 28, 181-196.

De la Cruz, R., Suárez, M., Belmar, M., Quiroz, D., Bell, M. 2003a. Geología del Área Coihaique-Balmaceda, Región Aisén del General Carlos Ibáñez del Campo. Carta Geológica de Chile, Ser. Geol. Básica 80, 40p., scale 1:100.000, Serv. Nac. de Geol. y Minería, Santiago, Chile.

De la Cruz, R., Suárez, M., Morata, D., Espinoza, F., Troncoso, A. 2003b. El Cenozoico del Lago General Carrera, Aysén, Chile (46º30'-47º15'S): estratigrafía y tectónica, in: X Congreso Geológico Chileno. Concepción.

De la Cruz, R., Cortés, J. 2011. Geología del área oriental de la Hoja Puerto Cisnes, Región Aysén del Gral Carlos Ibáñez del Campo. Carta Geológica de Chile, Ser. Geol. Básica 127, 70 p., scale 1:250000, Serv. Nac. de Geol. y Minería, Santiago, Chile.

De la Cruz, R., Welkner, D., Suárez, M., Quiroz, D. 2004. Geología del área Oriental de la Hojas Cochrane y Villa O'Higgins, Región Aisén del General Carlos Ibáñez del Campo. Carta Geológica de Chile, Ser. Geol. Básica 85, 57 p., scale 1:250.000, Serv. Nac. de Geol. y Minería, Santiago, Chile.

De La Cruz, R., Suárez, M. 2006. Geología del área Puerto Guadal-Puerto Sánchez, Región Aisén del General Carlos Ibañez del Campo. Carta Geológica de Chile, Ser. Geol. Básica 95, 58 p., scale 1:100000, Serv. Nac. de Geol. y Minería, Santiago, Chile.

De la Cruz, R., Suárez, M. 2008. Geología del Área de Chile Chico-Río de Las Nieves, Región de Aisén del General Carlos Ibáñez del Campo. Carta Geológica de Chile, Ser. Geol. Básica 112, 67 p., scale 1:100.000, Serv. Nac. de Geol. y Minería, Santiago, Chile.

Dunn, R.E., Strömberg, C.A., Madden, R.H., Kohn, M.J., Carlini, A.A. 2015. Linked canopy, climate, and faunal change in the Cenozoic of Patagonia. Science 347, 258-261.

Echaurren, A., Folguera, A., Gianni, G., Orts, D., Tassara, A., Encinas, A., Gimenez, M., Valencia, V. 2016. Tectonic evolution of the North Patagonian Andes (41°-44°S) through recognition of syntectonic strata. Tectonophysics 677–678, 99–114.

Escosteguy, L., Dal Molin, C., Franchi, M., Geuna, S., Lapido, O. 2002. Estratigrafía de la cuenca de los ríos El Zeballos y Jeinemeni, Noroeste de la provincia de Santa Cruz, in: XV Congreso Geológico Argentino. El Calafate.

Ecosteguy, L., Dal Molín, C., Franchi, M., Geuna, S., Lapido, O. 2003. Hoja Geológica 4772-II, Lago Buenos Aires, Provincia de Santa Cruz. Boletín del Servicio Geológico Argentino 339, scale 1:250.000, Programa Nacional de Cartas Geológicas de la República Argentina.

Encinas, A., Le Roux, J.P., Buatois, L.A., Nielsen, S.N., Finger, K.L., Fourtanier, E., Lavenu, A. 2006. Nuevo esquema estratigráfico para los depósitos marinos mio-pliocenos del área de Navidad (33º00'-34º30'S), Chile central. Rev. Geol. Chile 33, 221-246. https://dx.doi.org/10.4067/S0716-02082006000200002

Encinas, A., Pérez, F., Nielsen, S.N., Finger, K.L., Valencia, V., Duhart, P. 2014. Geochronologic and paleontologic evidence for a Pacific–Atlantic connection during the late Oligocene–early Miocene in the Patagonian Andes (43–44 S). J. South Am. Earth Sci. 55, 1-18.

Encinas, A., Folguera, A., Oliveros, V., Del Mauro, L.D.G., Tapia, F., Riffo, R., Hervé, F., Finger, K.L., Valencia, V.A., Gianni, G., Álvarez, O. 2015. Late Oligocene–early Miocene submarine volcanism and deep-marine sedimentation in an extensional basin of southern Chile: Implications for the tectonic development of the North Patagonian Andes. Geol. Soc. Am. Bull.128, 807-823.

Encinas, A., Folguera, A., Litvak, V.D., Echaurren, A., Gianni, G., Fernández Paz, F., Bobe, R., Valencia, V. 2016. New age constraints for the Cenozoic deposits of the Patagonian Andes and the Sierra de San Bernardo between 43° and 46°S, in: Primer simposio de tectónica sudamericana. Santiago, pp. 140.

Espinoza, F., Morata, D., Pelleter, E., Maury, R.C., Suárez, M., Lagabrielle, Y. Polvé, M., Bellon, H., Cotten, J., De la Cruz, R., Guivel, C. 2005. Petrogenesis of the Eocene and Mio–Pliocene alkaline basaltic magmatism in Meseta Chile Chico, southern Patagonia, Chile: Evidence for the participation of two slab windows. Lithos 82, 315-343.

Espinoza, F., Morata, D., Polve, M., Lagabrielle, Y., Maury, R.C., de la Rupelle, A., Guivel, C., Cotten, J., Bellon, H., Suarez, M. 2010. Middle Miocene calc-alkaline volcanism in Central Patagonia (47·S): petrogenesis and implications for slab dynamics. Andean Geol. 37, 300-328.

Flint, S.S., Prior, D.J., Agar, S.M., Turner, P. 1994. Stratigraphic and structural evolution of the Tertiary Cosmelli Basin and its relationship to the Chile triple junction. J. Geol. Soc. 151, 251-268.

Flynn, J.J., Marshall, L., Guerrero, J., Salinas, P. 1989. Geochronology of middle Miocene (Friasian Land Mammal Age) faunas from Chile and Colombia. Geological Society of America 21, p. A133

Flynn, J.J., Swisher III, C.C. 1995. Cenozoic South American land mammal ages: correlation to global geochronologies, in: Berggren, W.A., Kent, D.V., Aubry, M.P., Hardenbol, J. (Eds.), Special Publication 54. SEPM, Tulsa, pp. 317–333.

Flynn, J.J., Novacek, M.J., Dodson, H.E., Frassinetti, D., McKenna, M.C., Norell, M.A., Sears, K.E., Swisher, C.C., Wyss, A.R. 2002. A new fossil mammal assemblage from the southern Chilean Andes: implications for geology, geochronology, and tectonics. J. South Am. Earth Sci. 15, 285-302.

Flynn, J.J., Croft, D.A., Charrier, R., Wyss, A.R., Hérail, G., García, M. 2005. New Mesotheriidae (Mammalia, Notoungulata, Typotheria), geochronology and tectonics of the Caragua area, northernmost Chile. J. South Am. Earth Sci. 19, 55-74.

Folguera, A., Iannizzotto, N.F. 2004. The lagos La Plata and Fontana fold-and-thrust belt: long-lived orogenesis at the edge of western Patagonia. J. South Am. Earth Sci. 16, 541-566.

Folguera, A., Encinas, A., Alvarez, O., Orts, D., Gianni, G., Echaurren, A., D. Litvak, V., Navarrete, C., Sellés, D., Tobal, J., Ramos, M., Fennell, L., Fernández, L., Giménez, M., Martínez, P., Ruiz, F., Iannelli, S., 2018. Chapter 19. Neogene growth of the Patagonian Andes. Folguera, A., Contreras Reyes, E., Heredia, N., Encinas, A., Oliveros, V., Dávila, F.,

Collo, G., Giambiagi, L., Naipauer, M., Maksymowicz, A., Alvarez, O. (Eds.). The evolution of the Chilean-Argentinean Andes. Springer. doi.org/10.1007/978-3-319-67774-3_20

Forsythe, R., Nelson, E. 1985. Geological manifestations of ridge collision: Evidence from the Golfo de Penas-Taitao Basin, southern Chile. Tectonics 4, 477-495.

Franchi, M., Madden, R., Mazzoni, M., Swisher, C. 1995. Stratigraphy and geochronology of the mammal-bearing middle Miocene "Friasian" of Patagonia. J. S. Am. Earth Sci..

Frassinetti, D., Covacevich, V. 1999. Invertebrados fósiles marinos de la Formación Guadal (Oligoceno Superior-Mioceno Inferior) en Pampa Castillo, Región de Aisén, Chile.Subdirección Nacional de Geología, Sernageomín 51, 96.

Gianni, G., Navarrete, C., Orts, D., Tobal, J., Folguera, A., Giménez, M. 2015. Patagonian broken foreland and related synorogenic rifting: The origin of the Chubut Group Basin. Tectonophysics 649, 81-99.

Gianni, G., Echaurren, A., Folguera, A., Likerman, J., Encinas, A. , García, H.P.A., Dal Molin, C., Valencia, V. A. 2017. Cenozoic intraplate tectonics in Central Patagonia: Record of main Andean phases in a weak upper plate. Tectonophysics 721, 155-166. DOI 10.1016/j.tecto.2017.10.005

González, R. 1967. Geología de la región de Lago Blanco y Paso Río Mayo (Chubut). Acta Geológica Lilloana IX, 45-65.

González, R. 1978. Descripción Geológica de las Hojas 49a, Lago Blanco y 49b, Paso Río Mayo, Provincia del Chubut. SEGEMAR, Boletín 154–155, p. 45, Instituto de Geología y Recursos Minerales, Buenos Aires.

González Ruiz, L., Reato, A., Cano, M., Martínez, O. 2017. Old and new specimens of a poorly known glyptodont from the Miocene of Patagonia and their biochronological implications Acta Paleontológica Polónica. In Press.

Gorring, M.L., Kay, S.M., Zeitler, P.K., Ramos, V.A., Rubiolo, D., Fernandez, M.I., Panza, J.L. 1997. Neogene Patagonian plateau lavas: continental magmas associated with ridge collision at the Chile Triple Junction. Tectonics 16, 1-17.

Guillaume, B., Martinod, J., Husson, L., Roddaz, M., Riquelme, R. 2009. Neogene uplift of central eastern Patagonia: dynamic response to active spreading ridge subduction?. Tectonics 28, TC2009, doi:10.1029/2008TC002324.

Guillaume, B., Gautheron, C., Simon-Labric, T., Martinod, J., Roddaz, M., Douville, E. 2013, Dynamic topography control on Patagonian relief evolution as inferred from low temperature thermochronology, Earth Planet. Sc. Lett. 364, 157-167.

Guivel, C., Lagabrielle, Y., Bourgois, J., Maury, R.C., Fourcade, S., Martin, H., Arnaud, N. 1999. New geochemical constraints for the origin of ridge-subduction-related plutonic and volcanic suites from the Chile Triple Junction (Taitao Peninsula and Site 862, LEG ODP141 on the Taitao Ridge). Tectonophysics 311, 83-111.

Guivel, C., Morata, D., Pelleter, E., Espinoza, F., Maury, R.C., Lagabrielle, Y.,Polvé, M., Bellon, H., Cotten, J., Benoit, M., Suárez, M. 2006. Miocene to Late Quaternary Patagonian basalts (46–47 S): geochronometric and geochemical evidence for slab tearing due to active spreading ridge subduction. J. Volcanol. Geoth. Res. 149, 346-370.

Haschke, M., Sobel, E., Blisniuk, P., Strecker, M., Warkus, F. 2006a. Continental response to active ridge subduction. Geophysical Research Letters 33, L15315, doi: 10.1029/2006GL025972, 2006b.

Haschke, M., Günther, A., Melnick, D., Echtler, H., Reutter, K. J., Scheuber, E., & Oncken, O. 2006b. Central and southern Andean tectonic evolution inferred from arc magmatism, in: Oncken, O., Chong, G., Franz, G., Giese, P., Götze, H-J., Ramos, V.A., Strecker, M.A., Wigger, P. (Eds), The Andes. Springer Berlin Heidelberg, pp. 337-353

Herman, F., Brandon, M. 2015. Mid-latitude glacial erosion hotspot related to equatorial shifts in southern Westerlies. Geology 43, 987-990.

Hervé, F., Greene, F., Pankhurst, R.J. 1994. Metamorphosed fragments of oceanic crust in the upper Paleozoic Chonos accretionary complex, southern Chile. J. South Am. Earth Sci. 7, 263-270.

Hervé, F., Pankhurst, R.J., Drake, R., Beck, M.E. 1995. Pillow metabasalts in a mid-Tertiary extensional basin adjacent to the Liquiñe-Ofqui fault zone: the Isla Magdalena area, Aysén, Chile. J. South Am. Earth Sci. 8, 33–46.

Hervé, F., Sanhueza, A., Silva, C., Pankhurst, R.J., Fanning, M.C., Campbell, H., Crundwell, M. 2001. A Neogene age for Traiguén Formation, Aysén, Chile, as revealed by shrimp U-Pb dating of detrital zircons, in: III Simposio Sudamericano de Geología Isotópica. Pucón, pp. 570–574,

Horton, B.K., Fuentes, F. 2016. Sedimentary record of plate coupling and decoupling during growth of the Andes. Geology 44, 647-650.

Jordán, T.E., Isacks, B.L., Allmendinger, R.W., Brewer, J.A., Ramos, V.A., Ando, C.J. 1983. Andean tectonics related to geometry of subducted Nazca plate. Geol. Soc. Am. Bull. 94, 341-361.

Jordan, T., Matthew, W., Veiga, R., Pángaro, F., Copeland, P., Kelley, S., Mpodozis, C. 2001. Extension and basin formation in the southern Andes caused by increased convergence rate: a mid-Cenozoic trigger for the Andes. Tectonics 20, 308–324.

Kay, S.M., Ramos, V.A., Marquez, M. 1993. Evidence in Cerro Pampa volcanic rocks for slab-melting prior to ridge-trench collision in southern South America. J. Geol. 101, 703-714.

Kay, S.M., Copeland, P. 2006. Early to middle Miocene backarc magmas of the Neuquén Basin: Geochemical consequences of slab shallowing and the westward drift of South America. Geol. Soc. Am. 407, 185–213.

Lagabrielle, Y., Suárez, M., Rossello, E.A., Hérail, G., Martinod, J., Régnier, M., de la Cruz, R. 2004. Neogene to Quaternary tectonic evolution of the Patagonian Andes at the latitude of the Chile Triple Junction. Tectonophysics 385, 211-241.

Lagabrielle, Y., Suarez, M., Malavieille, J., Morata, D., Espinoza, F., Maury, R.C., Scalabrino, R., Barbero, L., de la Cruz, R., Rossello, E., Bellon, H. 2007. Pliocene extensional tectonics in the Eastern Central Patagonian Cordillera: geochronological constraints and new field evidence. Terra Nova 19, 413-424.

Lamb, S., Davis, P. 2003. Cenozoic climate change as a possible cause for the rise of the Andes. Nature 425, 792-797.

Ludwig, K.R. 2003. Isoplot 3.0-A geochronological toolkit for Microsoft Excel: Berkeley Geochronology Center Special publication 4, 71 p.

Madden, R. H., Guerrero, J., Kay, R. F., Flynn, J. J., Swisher III, C. C., Walton, A. H. 1997. The Laventan Stage and Age, in: Kay. R. F., Madden, R. H., Cifelli, R. H., Flynn, J. J. (Eds.), Vertebrate Paleontology in the Neotropics: The Miocene Fauna of La Venta, Colombia. Smithsonian Institution Press, Washington, D.C., pp. 499–519.

Martinod, J., Husson, L., Roperch, P., Guillaume, B., Espurt, N. 2010. Horizontal subduction zones, convergence velocity and the building of the Andes. Earth Planet. Sci. Lett. 299(3), 299-309.

Marshall, L. 1990. Fossil Marsupialia from the type Friasian land mammal age (Miocene), Alto Río Cisnes, Aisen, Chile. Rev. Geol. Chile 17(1), 19-55.

Marshall, L., Salinas, P. 1990. Stratigraphy of the Río Frías Formation (Miocene), along the Alto Río Cisnes, Aisen, Chile: Rev. Geol. Chile 17(1), 57-87.

Mercer, J. H., Sutter, J. F. 1982. Late Miocene-earliest Pliocene glaciation in southern Argentina: implications for global ice-sheet history. Palaeogeography, Palaeoclimatology, Palaeoecology 38(3-4), 185 - 206.

Miller, K. G., Fairbanks, R. G., Mountain, G. S. 1987. Tertiary oxygen isotope synthesis, sea level history, and continental margin erosion. Paleoceanography 2(1), 1-19.

Morata, D., de la Cruz, R., Suárez, M. 2005. The Bandurrias gabbro: Late Oligocene alkaline magmatism in the Patagonian Cordillera. J. S. Am. Earth Sci. 18, 147-162.

Mpodozis, C., Ramos, V. 1990. The Andes of Chile and Argentina, in: Ericksen, G., Cañas, M., Reinemund, J. (Eds.), Geology of the Andes and its relation to hydrocarbon and mineral resources: Circum-Pacific Council for Energy and Mineral Resources. Earth Sci. Series 11, pp: 59–88.

Mpodozis, C., Hervé, M., Nassi, C., Soffia, J. M., Forsythe, R. D., Nelson, E. P. 1985. El magmatismo plioceno de Península Tres Montes y su relación con la evolución del Punto Triple de Chile Austral. Rev. Geol. Chile 25–26, 13–28.

Muñoz, J., Troncoso, R., Duhart, P., Crignola, P., Farmer, L., Stern, C. R. 2000. The relation of the mid-Tertiary coastal magmatic belt in south-central Chile to the late Oligocene increase in plate convergence rate. Rev. Geol. Chile 27, 177–203.

Niemeyer, R. H. 1975. Geología de la región comprendida entre el Lago General Carrera y el Río Chacabuco. Aisén". PhD Dissertation (unpublished), University of Chile, Departamento de Geología, 309 pp., Chile.

Niemeyer, H., Skarmeta, J., Fuenzalida, R., Espinoza, W. 1984. Hojas Península de Taitao y Puerto Aisén. Carta Geológica de Chile 60–61, 80p., Ser. Nac. Geol. y Minería, Santiago, Chile.

Ortiz-Jaureguizar, E., Cladera, G.A. 2006. Paleoenvironmental evolution of southern South America during the Cenozoic. J. Arid Environ 66, 498-532.

Orts, D. L., Folguera, A., Encinas, A., Ramos, M., Tobal, J.,Ramos, V. A. 2012. Tectonic development of the North Patagonian Andes and their related Miocene foreland basin (41º30′ - 43º S). Tectonics 31, 1-24.

Orts, D., Folguera, A., Gimenez, M., Ruiz, F., Rojas Vera, E., Lince Klinger, F. 2015. Cenozoic building and deformational processes in the North Patagonian Andes. J. Geodyn. 86, 26-41.

Palazzesi, L., Barreda, V. 2012. Fossil pollen records reveal a late rise of open-habitat ecosystems in Patagonia. Nat. Commun. 3, 1294.

Palazzesi, L., Barreda, V., Cuitiño, J., Guler, M., Tellería, M., Ventura Santos, R. 2014. The Patagonian Fossil pollen records indicate that Patagonian desertification was not solely a consequence of Andean uplift. Nat. Commun. 5, 3558. http://dx.doi.org/10.1038/ncomms4558.

Pardo Casas, F., Molnar, P. 1987. Relative motion of the Nazca (Farallon) and South American plates since late Cretaceous time. Tectonics 6, 233-248.

Paredes, J. M., Azpiroz, G., Foix, M. 2006. Tertiary tectonics and sedimentation in the Cerro Piedra Oíl Field (Golfo San Jorge Basin), Argentina, in: IV Congreso Latinoamericano de Scdimentología and XI Reunión Argentina de Scdimentología. San Carlos de Bariloche, pp. 163.

Paredes, J. M., Plazibat, S., Crovetto, C., Stein, J., Cayo, E., Schiuma, A. 2013. Fault kinematics and depocenter evolution of oil-bearing, continental successions of the Mina del Carmen Formation (Albian) in the Golfo San Jorge basin, Argentina. J. S. Am. Earth Sci. 46, 63-79.

Parras, A., Dix, G. R., Griffin, M. 2012. Sr-isotope chronostratigraphy of Paleogene– Neogene marine deposits: Austral Basin, southern Patagonia (Argentina). J. S. Am. Earth Sci. 37, 122-135.

Perkins, M. E., Fleagle, J. G., Heizler, M. T., Nash, B., Bown, T. M., Tauber, A., Dozo, M. T. 2012. Tephrochronology of the Miocene Santa Cruz and Pinturas Formations, Argentina. Early Miocene Paleobiology in Patagonia: High-Latitude Paleocommunities of the Santa Cruz Formation. Vizcaíno, SF, 23-40.

Ploszkiewicz, V., Ramos, V. 1977. Estratigrafía y tectónica de la Sierra de Payaniyeu (provincia del Chubut). Rev. Asoc. Geol. Arg. 32, 209-226.

Ray, F.M. 1996. Stratigraphical and structural evolution of Tertiary backarc basins in southern Chili. PhD Dissertation (unpublished), University of Liverpool, 208 pp., Reino Unido.

Ramos, V. 1976. Estratigrafía de los Lagos La Plata y Fontana, Provincia de Chubut, República Argentina, in: I Congreso Geológico Chileno, pp. A43-A64.

Ramos, V. A. 1981. Descripción Geológica de la Hoja 47 Ab-" Lago Fontana", Provincia Del Chubut. Carta Geológico-económica de la República Argentina 183, scale 1: 200.000, Serv. Geol. Nac.

Ramos, V.A. 1982. Las ingresiones pacíficas del Terciario en el Norte de la Patagonia, in: III Congreso Geológico Chileno. Concepción, Actas I(A), pp. 262-288.

Ramos, V. A. 1989. Andean foothills structures in northern Magallanes Basin, Argentina. AAPG Bull. 73(7), 887-903.

Ramos, V., Kay, S. M. 1992. Southern Patagonian plateau basalts and deformation: backarc testimony of ridge collisions. Tectonophysics 205, 261-282.

Ramos, V. A. 2005. Seismic ridge subduction and topography: Foreland deformation in the Patagonian Andes. Tectonophysics 399(1), 73-86.

Ramos, V. A., Ghiglione, M. C. 2008. Tectonic evolution of the Patagonian Andes. Develop. Quat. Sci. 11, 57-71.

Ramos, M. E., Tobal, J. E., Sagripanti, L., Folguera, A., Orts, D. L., Giménez, M., Ramos, V. A. 2015. The North Patagonian orogenic front and related foreland evolution during the Miocene, analyzed from synorogenic sedimentation and U/Pb dating ($\sim 42°$ S). J. S. Am. Earth Sci. 64, 467-485.

Rivas, H., Bostelmann, E., Le Roux, J., Ugalde, R. 2015. Fluvial facies and architecture of the late middle Miocene, Mayoan, deposits of Chilean Patagonia, in: XIV Congreso Geológico Chileno, Actas 1, pp. 812-815.

Roth, S. 1908. Beitrag zur Gliederung der Sedimentablagerungen in Patagonien und der Pampasregion. Neues Jahrbuch für Mineralogie, Geologie und Paläontologie 26, 92-150.

Savignano, E., Mazzoli, S., Arce, M., Franchini, M., Gautheron, C., Paolini, M., Zattin, M. 2016. (Un) Coupled thrust belt foreland deformation in the northern Patagonian Andes: new insights from the Esquel-Gastre sector (41° 30'–43° S). Tectonics.

Scalabrino, B. 2009. Déformation d'un continent au-dessus d'une dorsale océanique active en subduction. PhD Dissertation (unpublished), Université Montpellier (Sciences et Techniques du Languedoc), pp. 388, France.

Scalabrino, B., Lagabrielle, Y., De la Rupelle, A., Malavieille, J., Polvé, M., Espinoza, F., Morata, D., Suárez, M. 2009. Subduction of an active spreading ridge beneath Southern South America: A review of the Cenozoic geological records from the Andean foreland, Central Patagonia (46-47ºS), in: Lallemand, S., Funiciello, F., (Eds.), Subduction Zone Geodynamics. Frontiers in Earth Science. Springer-Verlag, Berlin, Heidelberg, pp. 227-246.

Scalabrino, B., Lagabrielle, Y., Malavieille, J., Dominguez, S., Melnick, D., Espinoza, F., Rossello, E. 2010. A morphotectonic analysis of central Patagonian Cordillera: Negative inversion of the Andean belt over a buried spreading center? Tectonics 29(2).

Schmitz, M. D., Bowring, S. A. 2001. U-Pb zircon and titanite systematics of the Fish Canyon Tuff: an assessment of high-precision U-Pb geochronology and its application to young volcanic rocks: Geochimica et Cosmochimica 65, 2571-2587.

Scillato-Yané, G. J., Vizcaíno, S. F., Carlini, A. A., De Iuliis, G. 1993. Sistemática y filogenia de los Tardigrada del Mioceno medio de Patagonia II: Megatherioidea. Ameghiniana 30, 112-113.

Sdrolias, M., Müller, R. D. 2006. Controls on back-arc basin formation. Geochemistry, Geophysics, Geosystems 7(4).

Seton, M., Müller, R.D., Zahirovic, S., Gaina, C., Torsvik, T., Shephard, G., Talsma, A., Gurnis, M., Turner, M., Maus, S., Chandler, M., 2012. Global continental and ocean basin reconstructions since 200 Ma. Earth Sci. Rev. 113, 212–270.

Silver, P. G., Russo, R. M., Lithgow-Bertelloni, C. 1998. Coupling of South American and African plate motion and plate deformation. Science 279(5347), 60-63.

Skarmeta, J. 1976. Evolución tectónica y paleogeográfica de los Andes Patagónicos de Aisén durante el Neocomiano, in: I Congreso Geológico Chileno, Actas 1, pp. 1-56, Santiago.

Sláma, J., Kosler, J., Condon, D. J., Crowley, J. L., Gerdes, A., Hanchar, J. M., Horstwood, M. S. A., Morris, G. A., Nasdala, L., Norberg, N., Schaltegger, U., Schoene, B., Tubrett, M. N., Whitehouse, M. J. 2008. Plesovice zircon - a new natural reference material for U-Pb and Hf isotopic microanalysis. Chem. Geol. 249(1-2), 1-35.

Somoza, R., Ghidella, M.E., 2012. Late Cretaceous to recent platemotions inwestern South America revisited. Earth Planet. Sci. Lett. 331, 152–163.

Stott, L. D., Webb, P. N. 1989. The Neogloboquadrina continuosa last appearance datum level in the South Pacific. Micropaleontology 63-71.

Suárez, M., De La Cruz, R., Bell, M. 2007. Geología del área Ñireguao-Baño Nuevo. Región de Aisén del General Carlos Ibáñez del Campo. Carta Geológica de Chile, 108, Serv. Nac. de Geol. y Minería, Santiago, Chile.

Suárez, M., De La Cruz, R., Etchart, H., Márquez, M., Fanning, M. 2015. Síntesis de la Cronología Magmática Meso-Cenozoica de Patagonia Central, Aysén, Chile: edades U-Pb SHRIMP, in: XIV Congreso Geológico Chileno, Chile.

Suarez, M., De La Cruz, R. 2000. Tectonics in the eastern central Patagonian Cordillera (45º 30′–47º 30′ S). J. Geol. Soc. 157(5), 995-1001.

Suárez, M., de la Cruz, R., Bell, C. M. 2000. Timing and origin of deformation along the Patagonian fold and thrust belt. Geological Magazine 137, 345–353.

Thomson, S. N., Hervé, F., Stöckhert, B. 2001. Mesozoic Cenozoic denudation history of the Patagonian Andes (southern Chile) and its correlation to different subduction processes. Tectonics 20, 693-711.

Thomson, N. 2002. Late Cenozoic geomorphic and tectonic evolution of the Patagonian Andes between latitudes 42ºS and 46ºS: an appraisal based on fission-track results from the transpressional intra-arc Liquiñe-Ofqui fault zone. Geol. Soc. Am. Bull. 114, 1159–1173.

Thomson, S., Brandon, M., Tomkin, J., Reiners, P., Vásquez, C., Wilson, N. 2010. Glaciation as a destructive and constructive control on mountain building. Nature 467, 213–317.

Troncoso, A., Suárez, M., De la Cruz, R., Palma-Heldt, S. 2002. Paleoflora de la 1816 Formacion Ligorio Márquez (XI Región, Chile) en su localidad tipo: Paleobotánica, edad e implicancias paleoclimáticas. Revista Geológica de Chile 29 (1), 113-135.

Ugalde, R., Bostelmann, E., Buldrini, K. E., Oyarzún, J. L. 2015. Lithofacies, architecture, and depositional environments of the Santa Cruz Formation in Chilean Patagonia.

Ugarte, F. R. E. 1956. El Grupo de Río Zeballos en el flanco occidental de la Meseta Buenos Aires (Provincia de Santa Cruz). Rev. Asoc. Geol. Arg. 11(3), 202-216.

Uyeda, S., Kanamori, H. 1979. Back-arc opening and the mode of subduction. J. Geophys. Res.: Solid Earth 84(B3), 1049-1061.

Valencia, V. A., Ruiz, J., Barra, F., Geherls, G., Ducea, M., Titley, S. R., Ochoa-Landín, L. 2005. U-Pb zircon and Re-Os molybdenite geochronology from La Caridad porphyry copper deposit: insights for the duration of magmatism and mineralization in the Nacozari District, Sonora, Mexico. Mineralium Deposita 40(2), 175-191.

Vucetich, M. G. 1994. La Fauna de roedores de la Formación Cerro Boleadoras (Mioceno Inferior?). Acta Geológica Leopoldesia 39(1), 365-374.

Wiedenbeck, M., Alle, P., Corfu, F., Griffin, W.L., Meier, M., Oberli, F., von Quadt, A., Roddick, J.C., Spiegel, W., 1995. Three natural zircon standards for U–Th–Pb, Lu–Hf, trace element and REE analyses. Geostandards Newsletter 19, 1-23.

Williams, I. S. 1998. U-Th-Pb geochronology by ion microprobe. Rev. Economic Geol. 7, 1–35.

Yáñez, G., Cembrano, J. 2004. Role of viscous plate coupling in the late Tertiary Andean tectonics. J. Geophys. Res.: Solid Earth 109(B2).

Highlights

We studied Neogene synorogenic strata in the Patagonian foredeep between 45 and 47°S

Older synorogenic successions have yielded 18.7-16.4 Ma (U-Pb)

Contractional deformation ended after ~12 Ma

Neogene shortening only lasted ~6 My

Neogene shortening ended 4.5 My before subduction of the Chile Ridge in South America